In Vitro studies of CD4+ T cell phenotype and function: protocol optimization

Author	Rindert Venema
Student number	S3662802
Master	Biomedical Sciences (Biology of Cancer and Immune System)
Examiner	Prof. Dr. Peter Heeringa
Project supervisors	Drs. Nanthicha Inrueangsri
Location	Vasculitis research group Department of Pathology and Medical biology University Medical Center Groningen
Start and end dates	December 6, 2021 – July 7, 2022

Abstract

Granulomatosis with polyangiitis is a chronic relapsing autoimmune disease characterized by inflammation of small- to medium- sized blood vessels and the presence of ANCAs. Problematic in the disease is that 10% of the patients relapse yearly and treatment has severe side-effects. Moreover, cumulative flares of disease increase the changes at irreversible organ damage that can eventually causes death. Activated T cells are thought to play important roles in the pathogenesis of GPA. Known is that there is a disbalance between Tregs and Tem cells, where the Treg population has been found to be dysfunctional and the Tem population to be expanded. Based upon preliminary data showing that the PIM-1 kinase was upregulated in $CD4^+$ T cell subsets of active and remission patients, we want to investigate the effects of Pim kinase inhibition on the viability, purity, cell proliferation and cytokine production of $CD4^+$ T cells *in vitro*. Therefore, we optimized $CD4^+$ T cell isolation, TCR receptor stimuli, the media composition, the media composition in combination with Pim inhibitors and several antibody panels to guarantee consistent and reliable results when performing *in vitro* studies of $CD4^+$ T cell phenotype and function. We found that isolating $CD4^+$ T cells from PBMCs isolated from fresh blood resulted in a higher yield of the isolated $CD4^+$ T cell fraction compared to isolating $CD4^+$ T cells from cryopreserved PBMCs. Moreover, it was estimated that the optimal concentration of TCR stimuli was a combination of 0.5 µg/ml of plate-bound anti-CD3 and 1 µg/ of soluble CD28/CD49d. Furthermore, we found no major differences in purity and viability between the non-serum supplemented medium X-VIVO compared to the supplemented media X-VIVO + 5% HS and RPMI + 10% FCS. However, a decrease in cell proliferation was found for the non-supplemented medium compared to the supplemented media. Lastly, we found that Pim kinase inhibitors decrease cell proliferation without affecting the viability and purity compared to the DMSO control. The panPim inhibitor AZD1208, which inhibits all 3 Pim kinase isoenzymes, shows a stronger decrease in cell proliferation compared to the Pim-1 kinase inhibitor TCS-PIM-1 1.

Keywords: GPA, $CD4^+$ T cells, Pim kinase inhibitors, viability, purity, cell proliferation

Contents

List of Abbreviations

AAV	ANCA-associated vasculitides
ANCAs	Anti-neutrophilic cytoplasmic autoantibodies
APC	Antigen presenting cell
BCL-6	B cell lymphoma 6
BFA	Brefeldin A
BSA	Bovine serum albumin
CaI	Calcium Ionophore
CCR	C-C chemokine receptor
CPD	Cell proliferation dye
CXCL8	C-X-C motif chemokine ligand 8
dFBS	Decomplemented fetal bovine serum
EDTA	Ethylenediaminetetraacetic acid
EGPA	Eosinophilic granulomatosis with polyangiitis
FACS	Fluorescent associated cell sorting
FCS	Fetal calf serum
FMO	Fluorescent minus one
FoxP3	Forkhead box P3
GPA	Granulomatosis with polyangiitis
IL	Interleukin
IFN-y	Interferon-y
IgG	Immunoglobulin G
MHC	Major histocompatibility complex
MPA	Microscopic polyangiitis
MPO	Myeloperoxidase
MS	Multiple sclerosis
NETs	Neutrophil extracellular traps
PBMCs	Peripheral blood mononuclear cells
PBS	phosphate buffered saline
Pim	Proviral integration site for Moloney murine leukemia virus
PMA	Phorbol 12-myristate 13-acetate
PR3	Proteinase 3
RA	Rheumatoid arthritis
ROS	Reactive oxygen species
sCD	Soluble cluster of differentiation
T-bet	T-box expressed in T cells
TCR	T cell receptor
Teff	T effector
Tem	T effector memory
Tfh	T follicular helper

T1D	Type 1 diabetes
TNFα	Tumor necrosis factor-α
Treg	Regulatory T cell
RORγt	RAR-related orphan receptor gamma
RT	Room Temperature
RPMI	Roswell Park Memorial Institute
Runx3	Runt-related transcription factor 3
STAT3	signal transducer and activator of transcription 3

1. Introduction

1.1 Background and relevant literature review

- **ANCA-associated vasculitis**

Vasculitis is a general term for a group of uncommon autoimmune diseases that are characterized by blood vessel inflammation, endothelial injury and tissue damage. As an autoimmune disease, vasculitis is caused by an attack of the affected individual's immune system against an autoantigen, however, the exact underlying etiology is unknown [1]. Depending on the size of the blood vessels, the organs affected and blood tests for autoantibodies in particular anti-neutrophilic-cytoplasmic-autoantibodies (ANCAs), the vasculitides can be divided in more specific subgroups [2]. One of these subgroups is called ANCA-associated vasculitides (AAV), in which the presence of ANCAs, as the name already suggests, is a hallmark [3].

AAV is a group of rare, necrotizing small- to medium-sized vessel vasculitis that commonly affect the kidneys and the upper and lower airways although any organ can be affected [1, 4]. AAV includes three distinct diseases; granulomatosis with polyangiitis (GPA), microscopic polyangiitis (MPA) and eosinophilic granulomatosis with polyangiitis (EGPA). However, based on histopathological and clinical manifestations EGPA is generally considered to constitute a different disease entity [3]. GPA and MPA are histopathologically and clinically more overlapping. Clinically GPA often presents with sinonasal disease, lower respiratory tract involvement, granulomatous inflammation and glomerulonephritis. Similar manifestations can be found in MPA although granulomatous inflammation is lacking and renal manifestations are usually more severe. Moreover, GPA patients predominantly have ANCAs directed against the enzyme proteinase 3 (PR3), whereas the majority of MPA patients predominantly have ANCAs directed against myeloperoxidase (MPO) [1]. Recently, studies have observed an increase in the prevalence of AAV to 300-421 cases per million [1]. Currently, the 5-year survival rate of AAV patients is around 70-80% due to the use of immunosuppressive therapies and improvement in diagnostic strategies leading to earlier diagnosis. Treatment of AAV can be divided into two phases; a first phase aiming at remission induction and a second phase aiming to maintain remission [1]. Drugs which are currently commonly used to induce remission are immunosuppressives such as glucocorticosteroids in combination with either cyclophosphamide or the more recently permitted for use rituximab, an anti-CD20 monoclonal antibody that depletes B cells via among others complement-mediated and antibody-mediated cytotoxicity [5]. Although proven to be effective, 10% of the patients in remission will still relapse yearly and 30-50% will be affected by relapses within 5 years [1, 6]. These relapses cumulatively increase the risk of irreversible organ damage, and therefore the risk of comorbidities and death [1] Additionally, repeated treatment with immunosuppressives increases the risk of severe adverse events. Therefore, many studies have been investigating potential biomarkers that can predict these relapses to stratify patients based on their risk for relapse. Low risk patients receiving less immunosuppressants, lowering the risk of adverse events and high risk patients receiving more immunosuppressants, preventing relapses. However, at the moment there are no such biomarkers translated to the clinic yet and clinicians still rely on clear markers of active inflammation and clinical parameter that make it difficult to precisely predict relapses compromising patient tailored treatment [7].

- **Immunogenesis and pathogenesis**

Why self-tolerance towards ANCA antigens is broken is unknown [3, 8]. One described risk factor by the field is the nasal carriage of *S. aureus* by nearly two thirds of GPA patients, who had an increased risk for relapse compared to non-carrier patients [9]. The mechanisms of self-tolerance can be divided into central and peripheral self-tolerance mechanisms. Central self-tolerance depends on the recognition of self-antigens in the generative lymphoid organs [8]. When an immature T cell binds major histocompatibility complex (MHC) class I, class II peptides or self-antigens expressed by antigen presenting cells (APCs) in the thymus with a high enough affinity, it will undergo a process called negative selection. When this is the case it will result in an apoptotic signal deleting the T cell from the T cell pool in the thymus [8, 10]. The same process happens in the bone marrow for B cells, however B cells can also change the specificity of their B cell receptor. Peripheral-self-tolerance comes into play when mature autoreactive lymphocytes have escaped central tolerance mechanisms and are circulating the body. Here, the autoreactive effector lymphocytes can be directly inactivated via mechanisms that include clonal deletion, immunological ignorance, induction of anergy and conversion into a regulatory cell type [8]. Regulatory cell types such as regulatory T and B cells are critical in maintaining peripheral self-tolerance by suppressing immune responses. Functional and numerical impairments of these regulatory cells can lead to autoimmunity [3, 8]. Both have been reported in AAV, however data are not always consistent [8].

When the self-tolerance mechanisms of the immune system fail, autoreactive B and T cells will be able to initiate an effector response that involves both innate and adaptive immune effector pathways [1, 3]. A central event in the early effector phase of AAV is the interaction between ANCAs, produced by autoreactive plasma cells, and neutrophils. Neutrophils are key players in the pathophysiology of AAV as these cells have PR3 and MPO stored in their primary granules. Initial exposure of neutrophils to low doses of pro-inflammatory cytokines such as interleukin-β (IL-β) and tumor necrosis factor-α (TNFα) causes translocation of ANCA-antigens to the cell surface. At the same time, the proinflammatory environment causes neutrophils adhesion to the microvascular endothelium [3]. Subsequent binding of ANCAs to the ANCA-antigens results in full neutrophil activation, resulting in the production of reactive oxygen species (ROS) and the release of their granular contents, including PR3 and MPO, into the microvascular environment. More recently, studies have shown that ANCA mediated neutrophil activation also activates that alternative complement pathway resulting in C5a-C5aR mediated inflammatory amplification loop that is amenable for therapeutic intervention [11]. Finally, studies have shown that ANCA can trigger the generation of neutrophil extracellular traps (NETs), in a process called NETosis. Originally, NETosis was described as a peculiar form of cell death in which neutrophils discharge nuclear chromatin decorated with granule proteins forming an extracellular web that traps and kills bacteria. Subsequently, it was shown that NETs can be induced not only by pathogens but also by autoantibodies, immune complexes, cytokines and chemokines. NETs are composed of decondensed chromatin threads that contain bactericidal proteins from the cytoplasm and granules, including PR3 and MPO [12, 13]. Moreover, PR3 and MPO present on the decondensed chromatin threads can be transferred to myeloid dendritic cells, which trigger the adaptive immune response, further stimulating the production of ANCAs [12, 14]. Ultimately, ANCA mediated triggering of the inflammatory processes described above causes necrotizing endothelial damage culmination into destruction of the underlying tissue [12].

At the microvascular wall, depositions of PR3 and MPO can also be presented to autoreactive effector T cells that start to secret additional pro-inflammatory cytokines. This causes recruitment of even more effector leukocytes, further amplifying the inflammatory response and aggravating tissue injury (fig-1). Over time, memory B and T cells will form that play a substantial role in the chronicity and relapses of AAV [1].

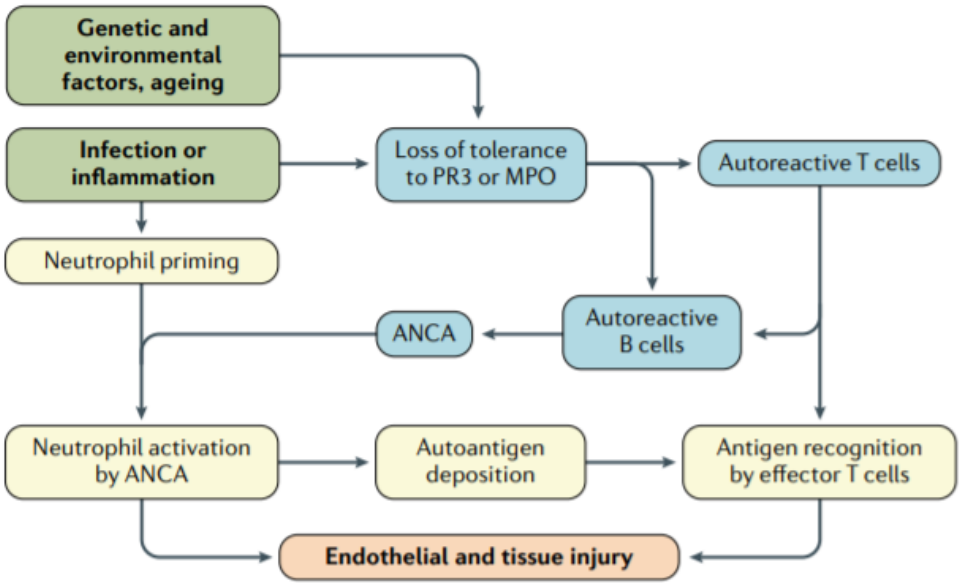

Fig 1.1 Simplified overview of pathogenetic events in GPA and MPA. Loss of self-tolerance and disease development is influenced by risk factors such as genetic and environmental factors, ageing, infection or inflammation (green). When loss of tolerance to PR3 or MPO occurs, autoreactive T and B cells will initiate an effector response leading to the production of ANCAs (blue). During the effector phase (yellow) neutrophils are primed, activated, and subsequently localize to the endothelial microvascular wall, causing tissue injury. Moreover, neutrophils deposit PR3 and MPO autoantigens at the microvascular site. Here, effector T cells recognize the autoantigen and start to produce pro-inflammatory cytokines. This causes the recruitment of more effector leukocytes, resulting in endothelial and tissue injury (orange) [1]. Adapted from Kitching et al., Nature reviews disease primer, 2020.

- **T cell aberrations in AAV**

There is considerable evidence that T cells are intimately involved in the pathogenesis of AAV. First, therapeutics targeting T cells in patients with refractory GPA as for instance antithymocyte globulin were able to induce remission, strongly indicating T cell involvement in the pathogenesis of AAV [15, 16]. Second, in MPO deficient mice immunized with MPO, depletion of CD4+ effector cells, achieved by anti-CD4 treatment, resulted in attenuation of the crescentic lesions and effector cell influx, without changes in ANCA titer [17]. Third, the vasculitic and granulomatous lesions in AAV patients contain abundant T cell infiltrates [18]. Finally, active and remission GPA patients show an increase in circulating T cells expressing cell surface markers for cellular activation compared to healthy controls, as well as an increase in soluble T cell activation markers as sCD25 and sCD30. High levels of these soluble markers have been shown to correlate with persistent ANCA or renewed ANCA positivity [19]. Another important indication for T cell involvement in the pathogenesis of AAV is the immunoglobulin G (IgG) isotype of the high-affinity ANCAs [20]. The commonly detected ANCA IgG isotypes, IgG1 and IgG4, indicate an isotype switch dependent on T follicular helper cells [1].

In AAV, functional and numerical aberrations in the CD4+ T helper cell population have been described, depending on the AAV phenotype (local or systemic) and disease activity. However, some observations are controversial [20]. For example, proportions of CD4+ CD25high CD127low regulatory T cell (Treg) subsets have been found to be to be decreased, unaltered or increased in active AAV patients [8]. There are multiple subsets of CD4+ T helper cells that can be characterized based on the cytokines they produce, transcription factors and surface markers they express, their ability to proliferate and their effector functions. CD4+ T helper subsets include among others; Th1, Th2, Th17, Th9, Th22, Treg, naïve T cells, T effector memory cells (Tem) and T follicular helper cells (Tfh). Each T helper cell population produces its own characteristic cytokines and expresses its own specific transcription factors, making it possible to distinguish the different populations in for instance patient blood samples [21]. As an example, Th1 cells can be defined by the production of cytokines as interferon- y (IFN-y) and IL-2, and the expression of the transcription factor T-box expressed in T cells (T-bet) [22]. This allows to study the T cell compartment at different stages of the disease (i.e. remission vs. active) and compare it to the T cell compartment of healthy donors.

Historically, many autoimmune diseases are either described as a Th1 dominant or Th2 dominant disease. Multiple sclerosis (MS), rheumatoid arthritis (RA) and type 1 diabetes (T1D) have for instance been described as Th1 dominant diseases, while allergy and atopy have been described as Th2 dominant diseases [23]. However, this is not as straightforward as it appears, since within autoimmune diseases themselves the dominant phenotype has been shown to be able to shift depending on the disease phenotype (local or systemic) or disease activity (active vs remission). In GPA this is the case as well [24]. In granulomatous lesions, GPA patients with localized disease were found to have a relative increase of cells expressing Th1-associated markers as CD26, IFN-y and C-C chemokine receptor type 5 (CCR5), while patients with systemic disease were found to predominantly express Th2-associated markers as IL-4 and CCR3. Similarities can be found in GPA patient's serum. Patients with localized disease had predominantly Th1-associated markers in their serum, while patients with generalized disease predominantly had Th2-associated markers in their serum [18]. Moreover, active GPA patients were found to have an increased production of IFN-y and normal levels of IL-4, which displays a Th1 cytokine profile [3]. In line with this is a study by Abdulahad et al., that described a predominance of the Th1 response during active and remission phase of GPA, however they did find a skewing in the CD4+ Tem population towards Th2 phenotype [25]. A later study by Abdulahad et al., showed that in response to PR3, the percentage of activated CD69, CD4+ T helper cells was significantly decreased compared to healthy control. Moreover, within this activated population there was found an increase in the percentage of Th2 cells and Th17 cells compared to healthy control, suggesting a polarization towards the Th2 response during remission [24]. Complementing this, is a study by Popa et al., that reported predominantly Th2-associated cytokines and low levels of IFN-y in the supernatant of peripheral blood mononuclear cells (PBMCs) from AAV remission patients stimulated with PR3 [26]. Additionally, Szczeklik et al., found an increase in cell count of peripheral Th2 cells in AAV remission patients, suggesting a polarization towards a Th2 response during remission [27].

Next to imbalances between Th1 and Th2 responses in AAV, the later discovered Th17 subset likely plays a prominent role in the pathogenesis of autoimmune diseases, including AAV [3, 28, 29]. Th17 cells produce IL-17, which has been shown to drive inflammation via the recruitment of neutrophils and macrophages. IL-17 stimulates the release of pro-inflammatory cytokines as IL-1B and TNF-a from macrophages. These cytokines can prime

neutrophils for activation by ANCA [19]. Moreover, IL-17 enhances autoantibody production and upregulates matrix metalloproteinases that degrade ECM causing tissue damage [30]. Furthermore, Th17 cells have a direct chemotactic effect on neutrophils via C-X-C motif chemokine ligand 8 (CXCL8) when activated [31]. This can recruit the neutrophils to vasculitic lesion, which is where Th17 cells have been identified in vasculitis [32]. However, a reciprocal relationship between Th17 cells and neutrophils was found. Neutrophils are also capable of inducing chemotaxis of Th17 cells, probably contributing to the accumulation of these cells at the inflammatory site in AAV [31]. Furthermore, Th17 show a high degree of plasticity, trans-differentiating into Th1, Th2, Treg and Tfh cells [33]. Several reports in AAV indicate that there is a skewing towards a Th17 response. Abdulahad et al., found that in vitro stimulation of PBMCs from GPA patients with PR3, resulted in increased expression levels of IL-17 and RAR-related orphan receptor gamma (RORyt) [24]. Moreover, Nogueira et al., found that Th17 cells are expanded in AAV patients during the active and remission phase of the disease [34]. Also elevated levels of IL-17 have been found in active GPA patients and these levels remained elevated when patients entered remission [27].

Equally important for AAV pathogenesis, is the disbalance between Tregs and Tem cells that has been reported by many research groups and reflected by a functional impairment of Tregs and a concomitant expansion of Tem cells [1, 3, 24, 35]. The expansion of Tem cells has been suggested to be caused by lack of control/suppression of the functionally impaired Tregs [15]. Abdulahad et al., showed that during remission the proportion of circulating CD4+ Tem cells increased in GPA patients [24]. However, during renal active disease a large proportion of circulating CD4+ Tem cells migrated to the inflammatory site, highlighting their significance in GPA pathogenesis [36]. The mechanisms responsible for the functional impairment of Tregs in AAV are still obscure but a number of possibilities have been suggested (reviewed in von Borstel et al.). These include Treg plasticity and differentiation into Th17 cells, reduced Treg responsiveness to IL-2, increased expression of forkhead box P3 (FoxP3) isoenzymes, and, different methylation patterns of the FoxP3 promoter [3]. Under inflammatory conditions, high levels of IL-6 stimulate the conversion of Tregs into Th17 cells, which stimulate the effector response in AAV. IL-6 has been shown to cause loss of suppressive functions of Tregs, as well as reducing the expression of Helios [37]. Helios is a transcription factor that is expressed in approximately 60-70% of the regulatory T cells and has been proposed as a robust marker for stable and highly suppressive Tregs in mice and humans [38]. Interestingly, RA patients treated with IL-6 receptor blocker Tocilizumab, showed an increased expression of circulating Helios+FoxP3+CD4+ T cells in comparison to RA patients receiving standard treatment without tocilizumab and healthy controls [39].

Lastly, also a disbalance in Tfh cells has been described in AAV [1, 39, 40]. Tfh express the lineage defining transcription factor B cell lymphoma 6 (BCL-6) and they are the predominant cell type producing IL-21 [41]. IL-21 is a key immune regulatory cytokine and experimental studies have demonstrated that blocking its expression either prevents or ameliorates autoimmune disease development. ANCA-positive GPA patients have increased percentages of IL-21 producing Tfh and increased expression of BCL-6 compared to ANCA-negative GPA patients and healthy controls. Moreover, it was found that IL-21 enhanced the production of ANCA and IgG in vitro upon CpG stimulation of PBMCs from GPA patients [39]. Furthermore, elevated serum IL-21 levels were reported in AAV patients with active disease compared to healthy controls that lowered upon immunosuppressive treatment [40].

In conclusion, aberrations in the T cell compartment are a characteristic feature of AAV patients (fig-2) not only during active disease but also in remission. However, currently, only few studies focus on restoring the balance of the T cell compartment in AAV mainly because the molecular mechanisms driving these aberrations are largely unknown.

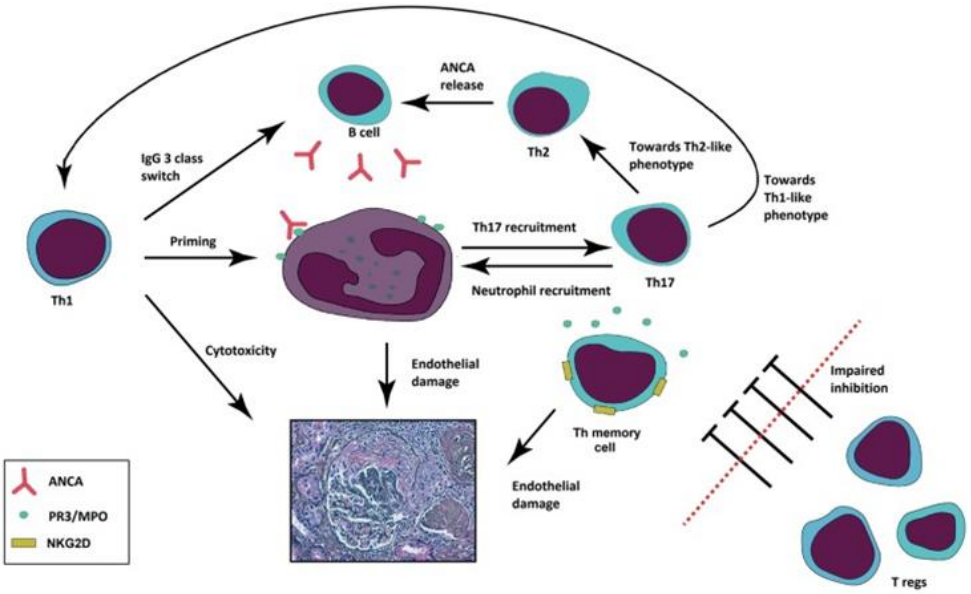

Fig 1.2 Overview of the role of T lymphocytes in AAV. The neutrophil is the key player in AAV. When neutrophils are primed by pro-inflammatory cytokines, autoantigens as PR3 and MPO translocated to the cell surface and displayed to ANCAs produced by autoreactive B cells. Binding of ANCA to these autoantigens results in full activation of the neutrophil causing the degranulation of neutrophilic granules that contain substances that promote endothelial damage and ongoing inflammation. Th1 responses prime neutrophils and cause isotype switching to IgG3 antibodies by B cells, which is the main antibody class in AAV. It is often predominant in localized disease. The Th2 response promotes ANCA production by B cells and is often predominant in more generalized disease. Th17 cells promote recruitment of neutrophils to the tissue and show a high degree of plasticity conveying Th1 and Th2 like phenotypes. Neutrophils, on the other hand, also have chemotactic effects on Th17 cells displaying a reciprocal relationship between these cells. Moreover, Tregs are dysfunctional in AAV, which hampers their ability to control the inflammatory process and prevent expansion of the Tem subset. Furthermore, numerical aberrations have been reported in the Treg subset. Additionally, Tfh cells also promote production of ANCAs by B cells. Lastly, the persistent exposure to ANCAs causes an expansion of the Th memory subset, which is particularly active and damaging when patients are relapsing. Adapted from L.M. Valenzuela et al., Clinical Kidney Journal, 2019.

1.2 Preliminary results of single-cell RNA-Seq data and Pim kinases in T cell functions

Proviral integration site for Moloney murine leukemia virus or Pim kinase is a serine threonine kinase proto-oncogene that has been studied in many types of cancers. Three homologous isoenzymes have been described, termed Pim-1, Pim-2 and Pim-3 [42]. Pim kinases were initially discovered in a screen for genes that could be virally inserted to enhance the development of lymphoma in the Eu-myctumor model [43]. Pim kinases are widely expressed in multiple cells and tissues, including vascular smooth muscle cells, lymphocytes, myocardial cells, prostate cells, and breast tissue. They are involved in the regulation of apoptosis, migration and cell proliferation. In cancer, Pim kinases are often upregulated and stimulate the migration, growth, proliferation and metabolism of malignant tumor cells [42].

There are several findings implicating the effects of Pim kinase inhibition on T cell differentiation. For instance, Pim-1 kinase, which is highly expressed in human Tregs, has been found to negatively regulate the activity of FoxP3 under inflammation by phosphorylating ser^{422}. High expression of Foxp3 is critical for maintaining Tregs suppressive function, and therefore also for limiting autoimmune responses. Pim-1 knockdown of in vitro expanded human Tregs resulted in FoxP3-induced gene expression and enhanced the immunosuppressive activity of the Tregs. Moreover, treatment of in vitro expanded primary Tregs with a Pim-1 specific inhibitor resulted in enhanced suppressive function of Tregs towards the proliferation of T effector (Teff) cells [44] In inflammatory bowel disease, Pim-1/3 inhibition prevents the proliferation of $CD4^+$ Tem cells and absence of Pim-1/3 activity withholds naïve $CD4^+$ T cells from fully differentiating into $CD4^+$ Tem cells in vitro and in vivo [45]. Moreover, in an experimental animal model of peanut-induced allergy, inhibition of Pim kinase resulted in attenuation of Th2 and Th17 differentiation, decreased Th2 and Th17 cytokine production and prevented intestinal inflammation through maintenance of the Runt-related transcription factor 3 (Runx3) of which Pim-1 kinase is an upstream regulator [46]. Furthermore, the Pim kinase family has been shown to promote Th1 differentiation, the production of IFN- y and upregulate T-bet and the IL-12/STAT4 signaling pathway during early Th1 differentiation [47]. Profoundly displaying the effects of Pim kinase inhibition on T cell differentiation is a recent paper by Maney et al. They found an upregulation of Pim-1 kinase in PBMCs from early RA patients, and specifically in the $CD4^+$ T cell subsets compared to healthy control. Therefore, they investigated the effect of the pan-Pim inhibitor AZD1208 and the Pim-1 inhibitor TCS-PIM-1 1 on the effector function of isolated $CD4^+$ T cells from these early patients. After 3 days of stimulation, $CD4^+$ T cells cultured with either Pim1 inhibitor or pan-Pim inhibitor showed a significant decrease in the activation marker CD25 and a significant decrease in proliferation, while there was no significant effect on cell viability. The decreases were sustained on day 6, with a minimal decrease in cell viability. After 6 days of culturing, the production of the Th1 specific cytokine IFN-y was significantly decreased for the $CD4^+$ T cells cultured with an inhibitor. This was also the case for the Th17 specific cytokine IL-17A, however only for the $CD4^+$ T cells treated with the Pim1 inhibitor. Interestingly, after 6 days of culturing also a significant increase was found in the frequency of $FoxP3^+$ cells and Tregs ($CD25^{high}FoxP3^+$) [48]. These findings implicate that Pim inhibitors could be beneficial for treatment an autoimmune disease as RA. Therefore, it is of great interest to see whether inhibition of Pim kinase can also be effective for treating other autoimmune diseases as AAV. Interestingly, recent single cell RNA-sequencing data on cryopreserved PBMCs of active GPA patients and healthy controls, performed by the ANCA vasculitis research group of the UMCG, demonstrated PIM1 and signal transducer and activator of transcription 3 (STAT3, an

upstream transcriptional regulator of Pim) upregulation in all $CD4^+$ T cell subsets. Moreover, qPCR analysis of bulk sorted $CD4^+$ Tnaive, $CD4^+$ Tem and $CD4^+$ Tregs of active and remission GPA patients confirmed elevated expression levels of PIM1 and STAT3 in all subsets in samples from active patients compared to those of healthy controls. Remarkably, Tem Pim1 kinase levels and Tem STAT3 levels were found to be still increased in a subgroup of remission patients suggesting that in clinical remission these patients' T cells are not quiescent. These data indicate that the STAT3/PIM1 signaling pathway is activated in T cells from GPA patients. Therefore, we aim to investigate the effect of Pim kinase inhibition on the activation, viability, proliferation, transcription factor expression levels and cytokine production of CD4+ T-helper cell subsets, in vitro, isolated from fresh blood of active GPA patients, remission GPA patients and healthy controls (fig 1.3). However, first protocol optimization is necessary to make sure everything works accordingly in our lab, as for instance the inhibitors. Furthermore, patient material in limited, which can be saved by optimizing the protocol first before starting the final experiment. Therefore, in this report we show how we optimized $CD4^+$ T cell isolation, the concentration of the TCR stimuli plate-bound anti-CD3 and soluble CD28/49d, the media composition for culturing $CD4^+$ T cells and the combination of media with Pim kinase inhibitors (fig 1.4).

1.3 Hypotheses

- Pim kinase inhibition does not affect the viability of $CD4^+$ T cells.
- Pim kinase inhibition decreases the proliferation and activation of $CD4^+$ T cells
- Pim kinase inhibition skews $CD4^+$T cells to decrease the production of Th1 and Th17 related cytokines
- Pim kinase inhibition increases the percentage of highly suppressive Treg cells

1.4 Objectives

- Optimize the $CD4^+$ T cell isolation procedure from fresh and thawed PBMCs.
- Optimize the concentrations of the TCR stimuli plate-bound anti-CD3 and soluble CD28/CD49d to study $CD4^+$ T cell activation and proliferation.
- Optimize the media composition for culturing $CD4^+$ T cells

1.5 Experimental design

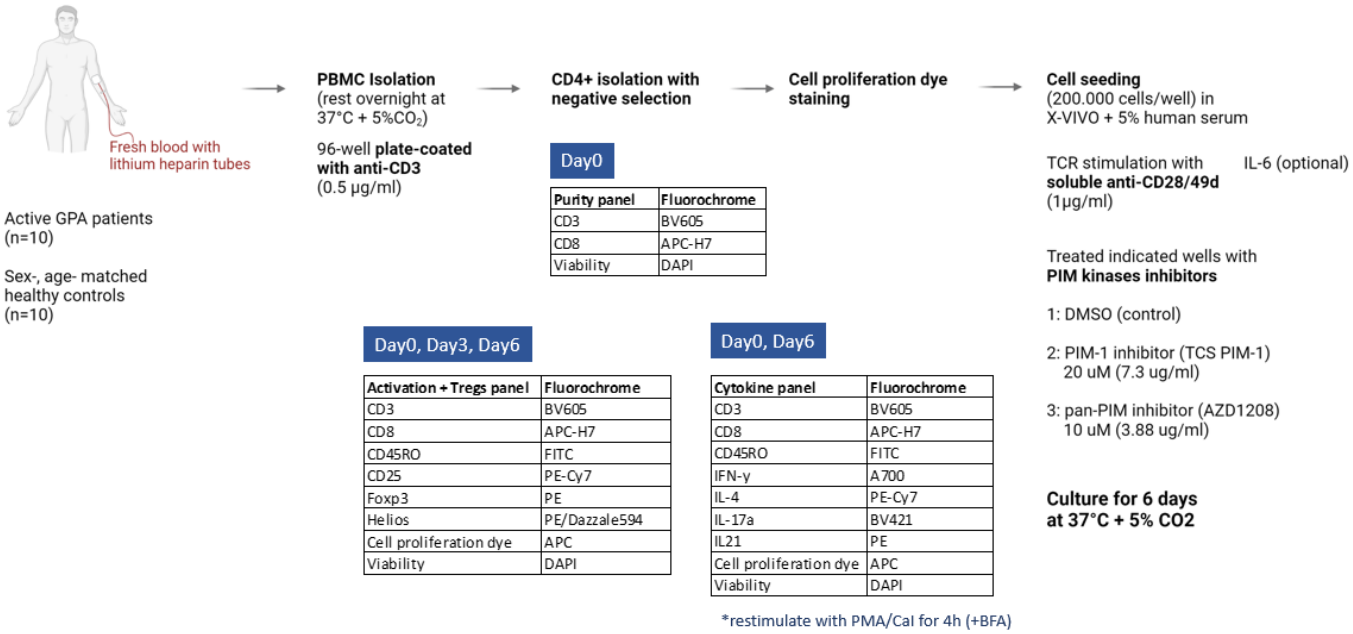

Fig 1.3 Graphical abstract experimental design Pim kinase study

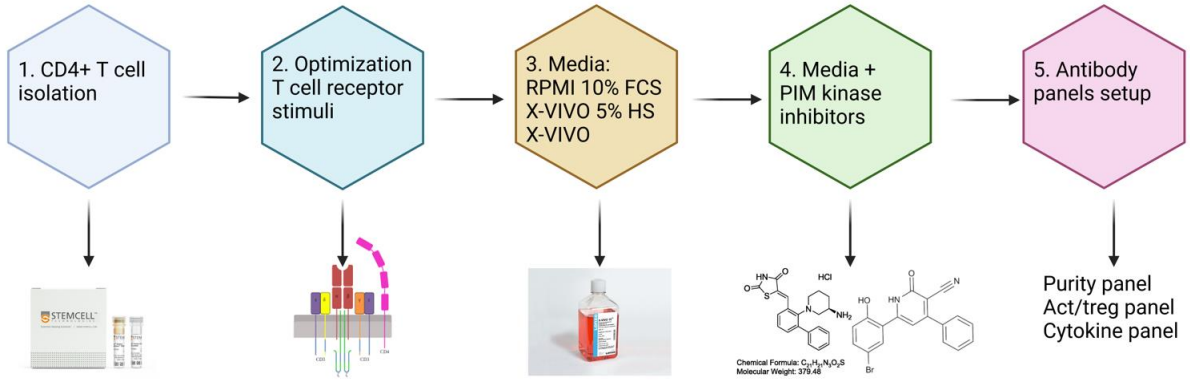

Fig 1.4 Overview of the protocol optimization performed

2. Materials and Methods

2.1 Cell isolation and culture

- **Isolation of PBMCs from fresh blood**

Heparinized blood was diluted 1:1 with phosphate buffered saline (PBS), pH 7.2 (Gibco) immediately after blood was drawn. PBMCs were prepared by density-gradient centrifugation of 4 ml of Lymphoprep (Axis-Shield PoC AS, Oslo, Norway) gently overlayed with 8 ml of the diluted blood. Afterwards, the top plasma layer was aspirated and the PBMC rings were collected. Next the PBMC rings were washed with PBS. After centrifugation, the PBMCs were pooled in 10 ml of PBS and subsequently counted using the coulter counter (Beckman Coulter) and centrifuged. Then, cells were either resuspended in X-VIVO complete medium (Lonza™ BioWhittaker™) and incubated overnight at 37°C 5% CO_2 or subjected to the $CD4^+$ T cells isolation procedure.

- **Isolation of $CD4^+$ T cells**

PBMCs were resuspended in cell separation buffer for $CD4^+$ T cell isolation, consisting of Ca^{++} and Mg^{++} free 1x PBS (Gibco, Paisley, UK) supplemented with 2% decomplemented fetal bovine serum (dFBS) of non-USA origin (Sigma-Aldrich, St. Louis, USA) and 1 mM ethylenediaminetetraacetic acid (EDTA) (Sigma-Aldrich) at a concentration of 5 x 10^7 cells/ml in a range of 0.25-2 ml. Human $CD4^+$ T cells were isolated from either thawed or freshly isolated PBMCs by negative magnetic selection according to the manufacturer's protocol of the EasySep ™ Human $CD4^+$ T Cell Isolation kit (Stemcell Technologies, Vancouver, Canada).

- **Thawing from cryopreserved PBMCs**

Cryo-preserved PBMCs were thawed in a 37°C water bath. Next the 1 ml of thawed PBMCs were collected in a volume of 10 ml of RPMI + 10% FCS and centrifuged. Then the supernatant was aspirated, after which the cells were resuspended in 10 ml of PBS and subsequently counted using the coulter counter. Then cells were either resuspended in X-VIVO complete medium or subjected to the $CD4^+$ T cells isolation procedure.

- **Cell culture and TCR-stimulated condition**

Freshly isolated $CD4^+$ T cells were cultured in serum free medium (X-VIVO™) at 200.000 cells per well in a polystyrene 96 wells flat bottom plate (Corning Incorporated, Corning, USA). and were stimulated with T cell receptor (TCR) stimuli plate-bound anti-CD3 (0.5 µg/ml) (OKT3; eBioscience) and soluble BD FastImmune™ CD28/CD49d (1 µg/ml) (BD Biosciences, Franklin Lakes, USA) for 3–6 days at 37°C with 5% CO_2. The coating with plate-bound anti-CD3 diluted in PBS was done 1 day prior to culturing, after which the coated plate was incubated for 2 hours at 37°C with 5% CO_2 and subsequently stored at 4 °C. Prior to culturing the anti-CD3 coated wells were washed 2x with PBS.

2.2 Purity and viability check of isolated human $CD4^+$ T cells

To assess viability, cells were harvested after 3 and 6 days of culturing. To collect as much cells as possible the wells were washed with PBS by pipetting up and down carefully. After harvesting, cells were washed by 2 ml of 1x PBS once and stained with Zombie UV™ Fixable Viability Dye (1:1000 dilution, Biolegend) for 15 min at room temperature (RT) in the dark. To

assess $CD4^+$ T cell purity, cells were subsequently washed with 2 ml of 1x PBS + 1% bovine serum albumin (BSA) (Sigma-Aldrich) and stained for the surface markers CD3 BV-605 (BD Biosciences) and CD8 APC-H7 (BD Biosciences) for 30 min at RT in the dark. Afterwards, cells were fixated using 1x BD FACS ™ lysing solution (BD Biosciences) diluted in demiwater (1:10) for 10 min at RT in the dark. Following, the cells were centrifuged and washed by 2 ml of 1x PBS + 1% BSA, after which they were resuspended in a total volume of ± 250 µl. Data was acquired on the BD FACSymphony™ A5 Cell Analyzer and analyzed by Kaluza 2.1 software (Beckman Coulter Life Sciences, Fullerton, USA) and FCS Express 6.0 software (DeNovo Software, Glendale, USA). The viability and purity was also checked on day 0 of the experiments called: the purity panel.

2.3 Staining cells with eFluor™ 670 proliferation dye for monitoring cell proliferation

To assess the proliferative capacity of the isolated $CD4^+$ T cells, cells were stained with Cell Proliferation Dye (CPD) eFluor™ 670 (Thermo Fisher Scientific, Carlsbad, USA) prior to culturing. Following the Stem cell $CD4^+$ T cell isolation procedure cells were washed twice with PBS and resuspended in PBS at 5 x 10^6 cells per 450 µl. Subsequently the cells were incubated for 5 min at 37 °C, after which they were stained with 1 mM CPD for 10 min at 37 °C, while gently mixing every 2 min. Labeling was stopped by adding 4-5 x the volume of Roswell Park Memorial Institute (RPMI) 1640 medium (Lonza, Basal, Switzerland) supplemented with 10% dFBS and 60 µg/ml Gentamycin Sulfate (GS) (Lonza) and incubating for 5 min on ice. Subsequently cells were washed twice with the same complete RPMI medium and washed twice with PBS. Next the cells were cultured and stimulated as described in section 2.1.

2.4 *In vitro* suppression of Pim kinases activity in CD4+ T cell

For the protein inhibition experiments, CD4+ T cells were isolated, cultured and stimulated as described in section 2.1, however in the presence of either the Pim1 kinase inhibitor (TCS PIM-1 1, also known as SC 204330; Tocris) (7.3 µg/ml), the Pan-Pim inhibitor AZD1208 (BioVision) (3.8 µg/ml), or an equivalent volume of DMSO as a control.

2.5 Characterization of $CD4^+$ T cell activation, viability, proliferation, and differentiation using flow cytometry

- **T cell activation marker and transcription factors of Tregs staining** *(act/Treg panel)*

Isolated human $CD4^+$ T cells were isolated, cultured and stimulated as described in section 2.1. CPD was stained as described in section 2.2 and viability was stained as described in section 2.2.3 Next, surface markers were stained with the following antibody-fluorochrome conjugates: CD3 BV-605 (BD Biosciences), CD8 APC-H7 (BD Biosciences), CD45RO FITC (BD Biosciences) and CD25-PE-CY7 (BD Biosciences) for 30 min at 4 °C. Afterwards, the Foxp3/Transcription Factor Staining Buffer Set eBioscience™ was used according to the protocol described in section 2.2.1 to block for unspecific binding and stain for transcription factors with the following antibody-fluorochrome conjugates: FoxP3-PE (eBioscience) and Helios-PE/Dazzle594 (Biolegend). Then, the cells were washed twice with Permeabilization Buffer and resuspended in ± 250 µl of PBS. Data was acquired on the BD FACSymphony™ A5 Cell Analyzer and analyzed by Kaluza 2.1 software and FCS Express 6.0 software.

- **Transcription factors staining to identify CD4$^+$ T cell subsets** *(TF panel)*

Isolated human CD4$^+$ T cells were isolated, cultured and stimulated as described in section 2.1. CPD was stained as described in section 2.2. Viability was stained with aqua fixable LIVE/DEAD™ dye BV510 (Invitrogen, ThermoFisher, USA), immediately following the last wash of the CPD staining protocol. First, the LIVE/DEAD dye was diluted in 1x PBS (1:4000) and afterwards the cells were stained with the dye for 30 min at 4 °C. Next, the cells were washed twice by 2 ml of 1x PBS + 1% BSA, after which they were resuspended in a total volume of ± 100 µl. Then, the cells were stained for the surface markers CD3 BV-605 (BD Biosciences), CD8 APC-H7 (BD Biosciences), CD45RO FITC (BD Biosciences), CD4 BUV-395 (BD Biosciences) for 30 min at 4 °C. Afterwards, the cells were washed with 2 ml of cold 1x PBS and fixed with freshly prepared Fix/Perm buffer (Foxp3/Transcription Factor Staining Buffer Set eBioscience™), (Fix/Perm Concentrate, Fix/Perm Diluent 1:4) for 45 min at 4 °C. After fixation, the cells were washed once with PBS. Next, they were washed twice with Permeabilization Buffer (Foxp3/Transcription Factor Staining Buffer Set eBioscience™), which was diluted to 1x with demi water and subsequently filtered with a syringe and 0.2 µm filter (Sartorius). After washing, the cells were resuspended in ± 100 µl of Permeabilization Buffer and incubated with normal mouse serum for 15 min at RT to block unspecific binding of the antibodies. Then, the cells were stained for transcription factors with the following antibody-fluorochrome conjugates: BCL6-BV421 (BD Biosciences), RORyT-PerCP-ef710 (eBioscience), FoxP3-PE (eBioscience), Helios-PE/Dazzle594 (Biolegend), Tbet-PE-CY7 (eBioscience) and Gata3-BV-711(BD Biosciences) for 30 min at RT. Next, the cells were washed twice with Permeabilization Buffer and resuspended in ± 250 µl of PBS. Data was acquired on the BD FACSymphony™ A5 Cell Analyzer and analyzed by Kaluza 2.1 software and FCS Express 6.0 software. The compensation setup with Fluorescent Minus One (FMO) controls and a detailed protocol can be found in supplementary section

- **Intracellular cytokines staining to identify CD4$^+$ T cell subsets** *(ICS panel)*

Isolated human CD4$^+$ T cells were isolated, cultured and stimulated as described in section 2.1. CPD was stained as described in section 2.2. After culturing the cells for 6 days, the cells were harvested as described in section 2.2 and stimulated with 25 ng/ml Phorbol 12-myristate 13-acetate (PMA) (Sigma-Aldrich), 0.8 µg/ml Calcium Ionophore (CaI) (Sigma-Aldrich) and 10 µg/ml Brefeldin A (BFA) (Sigma-Aldrich) at 37 °C + 5% CO_2 for 4 hours. As a negative control unstimulated cells were used treated with 10 µg/ml BFA. Afterwards, the cells were washed with 1x PBS and stained for viability as described in section 2.5 (TF panel). Then, cells were washed twice with 2 ml of 1x PBS + 1% BSA and stained the same surface markers as described in section 2.5 (TF panel) for 15 min at RT. Next, the cells were fixated with Reagent A fixation medium (Caltag) for 15 min, RT at dark, followed by a wash with PBS + 5% FCS. Continuing, the cells were permeabilized with Reagent B permeabilization medium (Caltag), and subsequently stained for intracellular cytokines with the following antibody-fluorochrome conjugates: IFN-y-A700 (BD Biosciences), IL-4-PE-Cy7 (BD Biosciences), IL-17-BV421 (Biolegend) and IL-21-PE (BD Biosciences), for 30 min, RT at dark. Afterwards, cells were washed with PBS + 5% FCS, and subsequently resuspended in ± 250 of this solution. Data was acquired on the BD FACSymphony™ A5 Cell Analyzer and analyzed by Kaluza 2.1 software and FCS Express 6.0 software.

2.6 Cell proliferation analysis

Multiple software packages analyzing cell proliferation give the same name to distinct cell proliferation statistics [49]. For instance, where FCS Express describes the proliferation index as the average number of cells an initial cell became, NovoExpress describes this as the expansion index. The frequency divided is described as the percentage of original cells that are divided in NovoExpress, however in FCS Express this is referred to as % divided. The proliferation index in NovoExpress is described as the sum of the number of divisions in each generation divided by the number of original cells that are divided, FCS express 6.0 does not provide a statistic reflecting this definition. An overview of the cell proliferation statistics and their definitions for both programs can be found in table 2.1. Also an important statistic of the cell proliferation data is the Reduced-Chi-Square, which gives an estimate of the "goodness of fit" of the model, where values below 5 indicate a good fit. In this study FCS Express 6.0 was used to investigate the optimal concentration of the TCR stimuli plate-bound anti-CD3 and soluble CD28/49d. NovoExpress was used to investigate the optimization of the media and optimization of the media in combination with inhibitors. NovoExpress was chosen for these optimization experiments because it had a better "goodness of fit" of the model, which translates into more reliable results.

Table 2.1 Cell proliferation statistics and their definitions for FCS Express and NovoExpress

FCS express	NovoExpress	Definition
Proliferation index	Expansion index	Average number of cells an initial cell became
% divided	Frequency divided	The percentage of cells that divided
Division index	Replication index	Average number of cells a dividing cell became
N/A	Proliferation index	Sum of the number of divisions in each generation divided by the number of original cells that are divided

2.7 Statistical analysis

Since this study has mostly been an optimization study until this point, there have not been involved any patients to preserve precious patient materials. Although, one experiment has been performed with an active patient vs. healthy control with the act/Treg panel and ICS panel. However, this experiment failed due to viability issues. After 3-6 days of culturing viability only ranged between approximately 5 and 35 %, and a substantial CD8 signal appeared on the FCS plots (probably due to sticky dead cells), even though they had been removed nearly all during negative selection of $CD4^+$ cells. Therefore, further optimization experiments were performed with blood of healthy controls. Optimization experiments performed in this particular study always have had n=1, which is why no statistical analysis could be performed. Therefore, data obtained by flow cytometry was analyzed by Kaluza, FCS express and NovoExpress software and arranged in figures. Furthermore, percentages gated can be observed in the figures and tables.

3. Results

3.1 Isolating CD4⁺ T cells from PBMCs isolated from fresh blood results in a higher yield of CD4⁺ T cells

A critical aspect when studying phenotype and function of isolated CD4⁺ T cells in vitro is the purity and viability of the isolated fractions. Since we used cryopreserved PBMCs we first determined the percentage of CD4⁺ T cells in these samples and found that approximately 45% of cell were CD4⁺ T cells (figure 3.1.1.)

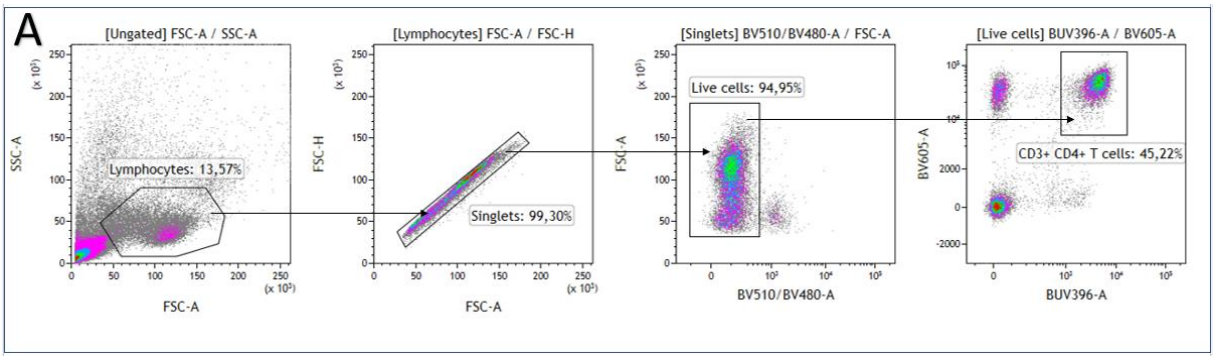

Fig. 3.1.1 Checking the percentage of CD3⁺CD4⁺ T cells in cryopreserved PBMCs (A, B, C, D) Representative gating strategy to check the viability and percentage of CD3⁺CD4⁺ T cells in cryopreserved PBMCs. (A) Lymphocytes gated based on SSC and FSC. (B) Single cells gated based on FSC-H and FSC-A. (C) Live cells gated by having a negative signal for LIVE/DEAD dye. (D) Percentage of CD3⁺CD4⁺ T cells in cryopreserved PMBCs.

Next, we used a negative magnetic selection kit (EasySep ™ Human CD4⁺ T Cell Isolation kit) to isolate CD4⁺ T cells. According to the manufacturer of the kit, a purity of 94.8 ± 2.3% should be reached after a single round of incubation. Here, after one round of incubation with a magnet from a different company (Beckton Dickinson), a purity of 97.23% (fig. 3.1.2A) with a cell viability of 99.33% was obtained. We also investigated whether multiple rounds of incubation with the magnet would increase the purity of the isolated human CD4⁺ T cells without affecting cell viability. Additional rounds of incubation did not further increase the purity nor did it affect cell viability (data not shown).

Next we aimed to determine whether we could increase the yield of the isolated CD4⁺ T cell fraction by rinsing the initial tube that was incubated in the magnet again with CD4⁺ T cell isolation buffer. Although this did not change the viability, it did decrease the purity of the isolated fraction.

Lastly, we investigated whether isolating human CD4⁺ T cells from either cryopreserved PBMCs or PBMCs isolated from fresh blood influenced the number, viability and purity of the isolated fraction of CD4⁺ T cells. Starting with approximately the same number of PBMCs (34.10^6 cryopreserved PBMCs vs 32.10^6 freshly isolated PBMCs) for CD4⁺ isolation yielded $1.79.10^6$ CD4⁺ T cells and $3.51\ 10^6$ CD4⁺ T cells for thawed and freshly isolated PBMCs respectively. Cell viability (98.62% vs 98.75%) and purity (95.97% vs 93.23%) were similar between thawed and fresh samples. Although the PBMCs isolated from fresh blood and the PBMCs isolated from cryopreserved PBMCs were not from the same donor, we observed the same difference in multiple experiments (data not shown).

3.2 Determination of the optimal concentration of TCR stimuli for CD4⁺ T cell expansion *in vitro*

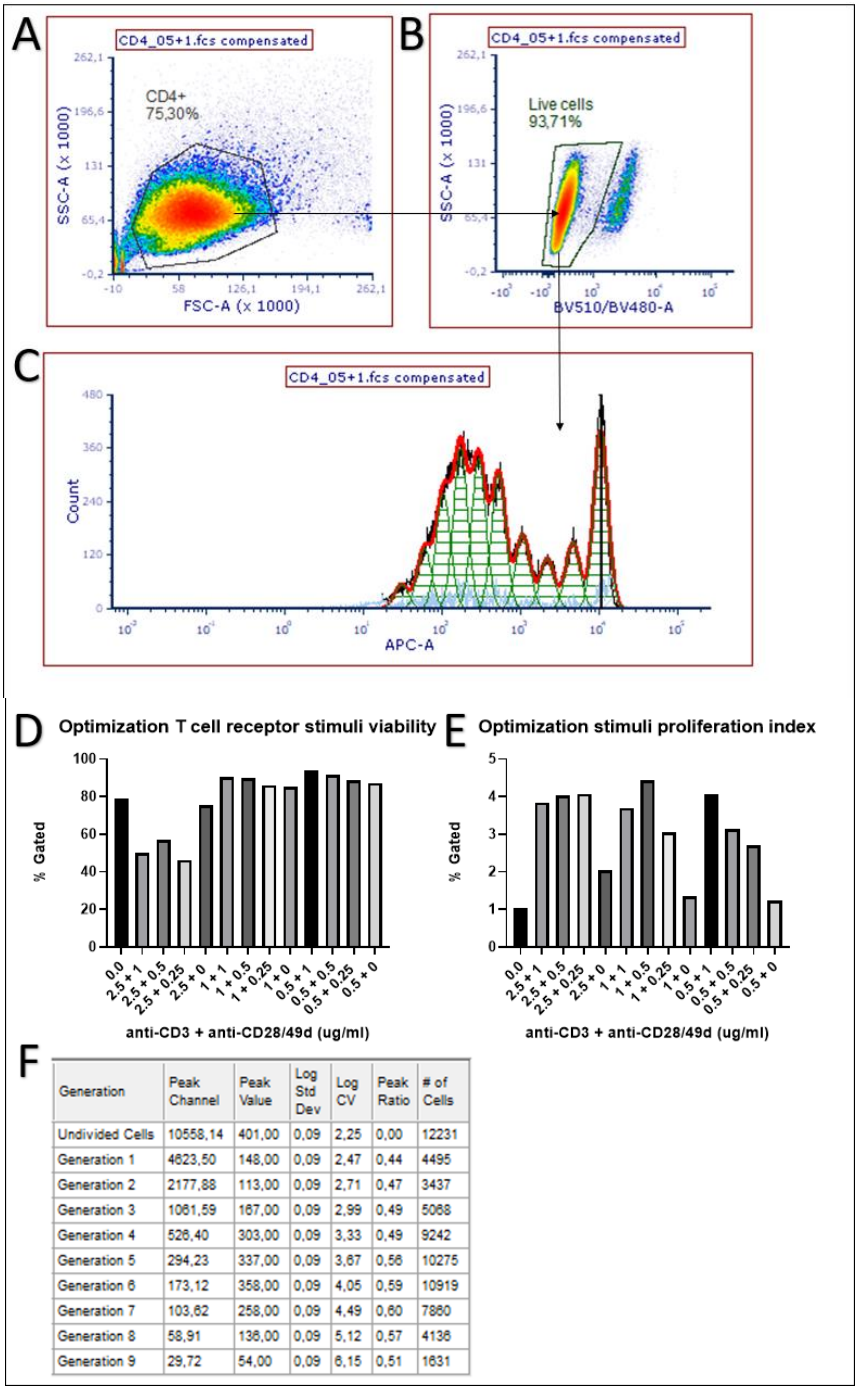

F

Generation	Peak Channel	Peak Value	Log Std Dev	Log CV	Peak Ratio	# of Cells
Undivided Cells	10558,14	401,00	0,09	2,25	0,00	12231
Generation 1	4623,50	148,00	0,09	2,47	0,44	4495
Generation 2	2177,88	113,00	0,09	2,71	0,47	3437
Generation 3	1061,59	167,00	0,09	2,99	0,49	5068
Generation 4	526,40	303,00	0,09	3,33	0,49	9242
Generation 5	294,23	337,00	0,09	3,67	0,56	10275
Generation 6	173,12	358,00	0,09	4,05	0,59	10919
Generation 7	103,62	258,00	0,09	4,49	0,60	7860
Generation 8	58,91	136,00	0,09	5,12	0,57	4136
Generation 9	29,72	54,00	0,09	6,15	0,51	1631

Fig 3.2 Optimization of T cell expansion *in vitro* culture by varying concentrations of anti-CD3 and anti-CD28/49d. (A, B, C) Representative gating strategy FCS express analysis optimization of anti-CD3 and anti-CD28/49d. First isolated CD4⁺ T cells are gated based on SSC and FSC (A). Second, live cells are gated based on being negative for LIVE/DEAD viability dye (B). Third, the live cell gate is used to plot a cell proliferation graph with each peak representing a generation of cells, with the green line representing the staring generation of undivided cells (C). Viability of isolated CD4⁺ T cells at various concentrations of anti-CD3 and anti-CD28/49d (D). Proliferation index of isolated CD4⁺ T cells at various concentrations of anti-CD3 and anti-CD28/49d (E). Undivided cells and cell generation 1-9 with statistics including Peak Channel, Peak Value, Log Std Dev, Log CV, Peak Ration and # of cells (F).

T cell activation, expansion and differentiation *in vitro* and *in vivo* needs 3 signals. Signal 1: activation of the TCR complex by anti-CD3, signal 2: co-stimulation via ligation of CD28 with CD80 or CD86, in our study mimicked by adding soluble anti-CD28, and signal 3: cytokines. Therefore, we determined the optimal concentrations of plate-bound anti-CD3 and soluble anti-CD28/49d. As shown in figure 3.2 the optimal combination of concentrations of plate-bound anti-CD3 and soluble anti-CD28/49d was estimated at 0.5 µg/ml of plate-bound anti-CD3 and 1 µg/ml of soluble anti-CD28/49d. With these concentrations cell viability was 93.71% (fig. 3.2B) after 6 days of culturing (fig. 3.2D) and $CD4^+$ T cells readily proliferated as indicated by a proliferation index of 4.05. (fig. 3.2D).

3.3 Medium supplementation with serum is necessary for optimal $CD4^+$ T cell expansion *in vitro*

To further optimize culturing conditions, we also investigated the influence of media composition on $CD4^+$ T cell activation and proliferation. Three different types of media were studied, RPMI + 10% FCS TCR, X-VIVO + 5% human serum TCR, and X-VIVO TCR, with regard to percentage of isolated $CD4^+$ cells, cell viability, cell purity (% of $CD3^+CD8^-$ cells), and cell proliferation. For the fresh samples, next to the optimized concentrations of TCR stimuli, we also included an unstimulated condition (table 3.1).

Table 3.1 Culturing conditions media experiment

Medium	Serum	TCR stimuli	condition
RPMI	10% FCS	Yes	Fresh
RPMI	10% FCS	No	Fresh
RPMI	10% FCS	Yes	Thaw
X-VIVO	5% HS	Yes	Fresh
X-VIVO	5% HS	No	Fresh
X-VIVO	5% HS	Yes	Thaw
X-VIVO	No	Yes	Fresh
X-VIVO	No	No	Fresh
X-VIVO	No	Yes	Thaw

After 3 days of culturing, we observed no major differences regarding cell viability and purity between the 3 different media compositions. However, a minor decrease in viability was found for each type of media for unstimulated cells compared to its TCR-stimulated cells (fig 3.3.1C & D). We observed that cell proliferation was decreased for the non-supplemented TCR-stimulation media (X-VIVO) compared to the serum-supplemented media, reflected by the frequency divided and the expansion index. After 3 days of culturing, the frequency divided (fig 3.3.2D) was decreased for the non-supplemented TCR-stimulation media (11.99%) compared to the serum-supplemented TCR-stimulation media (RMPI + 10% FCS; 35.60% and X-VIVO; 27.02%). The expansion index (fig 3.3.2 E) showed a similar trend; non-supplemented 1.24, compared to supplemented 1.84 (RPMI) and 1.65 (X-VIVO). The TCR-stimulation media

showed similar proliferation indices (fig 3.3.2 F). Hardly any cell proliferation was observed for the media without TCR stimuli.

After 6 days of culturing, we observed no major differences regarding the viability and purity between the 3 different types of TCR-stimulated media. However, a decrease in viability was found for unstimulated cells compared to TCR-stimulated cells for all media (fig 3.3.3C & D). Similar to day 3, we observed a decrease in the cell proliferation for the non-supplemented TCR-stimulated media. Again the frequency divided and expansion index were decreased for the non-supplemented TCR-stimulation media compared to the supplemented TCR-stimulation media (fig 3.3.4D & E). Furthermore, similar to day 3, hardly any cell proliferation was observed for the media without TCR stimuli (fig 3.3.4D, E & F).

Also for the $CD4^+$ T cells isolated from cryopreserved PBMCs we observed no major differences regarding the viability and purity for the 3 different media after 3 days of culturing (fig 3.3.5C & D). Similar to $CD4^+$ T cells isolated from PBMCs isolated from fresh blood, we observed a decrease in cell proliferation for the non-supplemented media compared to the supplemented media, however in this case only reflected by a decrease in the frequency divided (fig 3.3.6 D).

Similar to day 3, we observed no major differences in viability and purity between the 3 different media compositions (fig 3.3.7C & D). Furthermore, also on day 6 we observed a decrease in cell proliferation for the non-supplemented media compared to the supplemented media, which was again reflected by a decrease in the frequency divided but not the expansion index and proliferation index (fig 3.3.8 D, E & F)

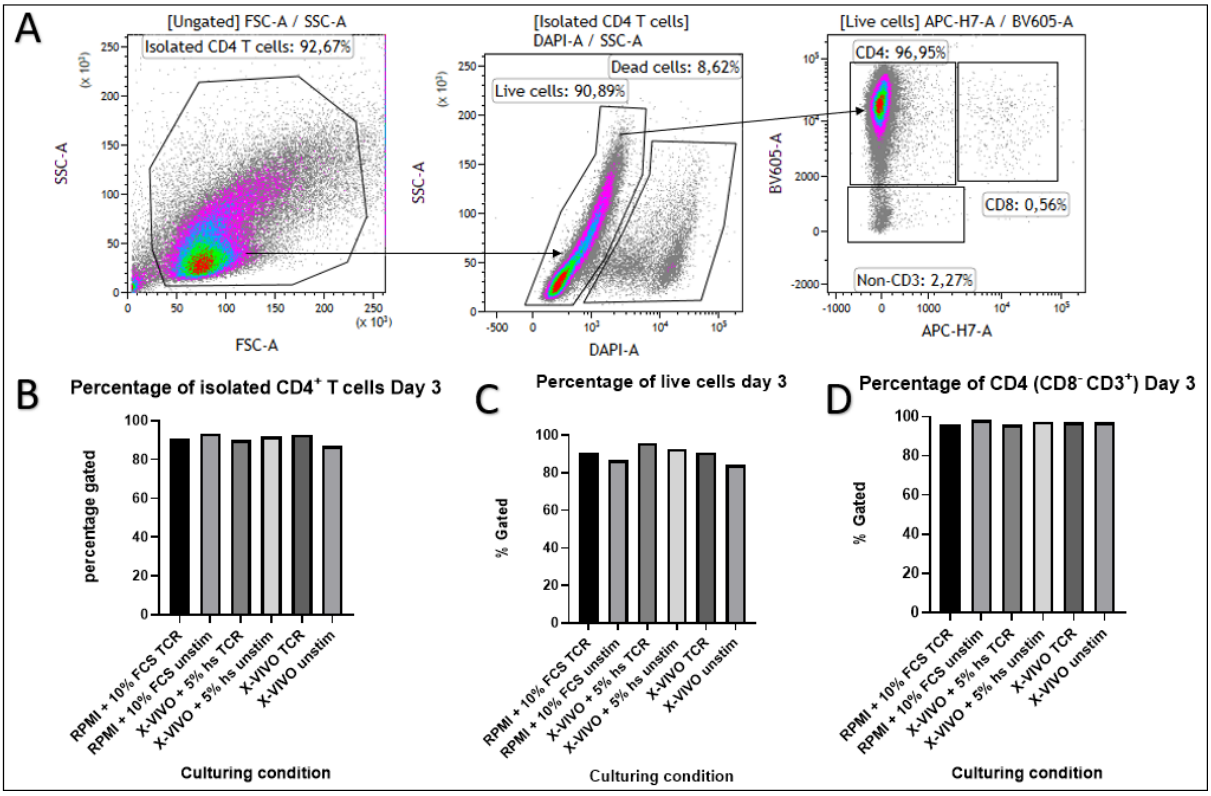

Fig 3.3.1 The effect of media composition on viability and purity of CD4⁺ T cell isolated from PBMCs isolated from fresh blood day 3. Representative gating strategy after 3 days of culturing CD4⁺ T cells isolated from PBMCs isolated from fresh blood (A). Percentage of isolated CD4⁺ T cells cultured for 3 days in various types of media compositions (B). Viability of CD4⁺ T cells cultured for 3 days in various types of media compositions (C). Purity of CD4⁺ T cells cultured for 3 days in various types of media compositions (D). Culturing conditions: RPMI + 10% FCS TCR, RPMI + 10% FCS unstimulated, X-VIVO + 5% human serum TCR, X-VIVO + 5% human serum unstimulated, X-VIVO TCR, X-VIVO unstimulated.

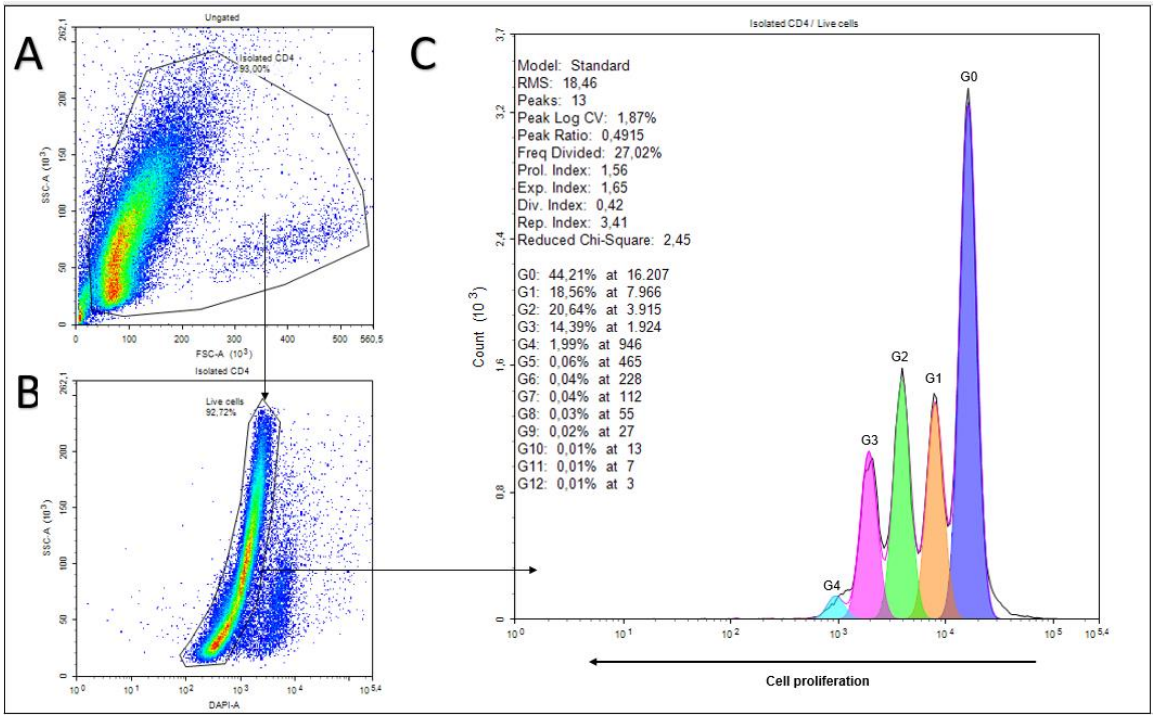

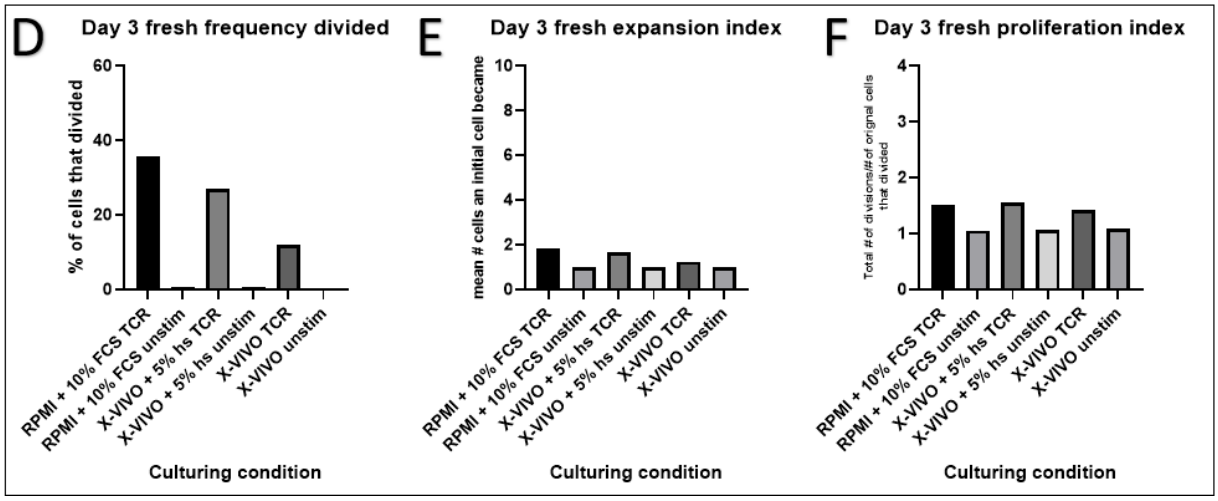

Fig 3.3.2 The effect of media composition on cell proliferation of CD4⁺ T isolated from PBMCs isolated from fresh blood day 3. Representative gating strategy after 3 days of culturing CD4⁺ T cells isolated from PBMCs isolated from fresh blood (A, B, C). Frequency divided of CD4+ T cells cultured for 3 days in various types of media compositions (D). Expansion index of CD4+ T cells cultured for 3 days in various types of media compositions (E). Proliferation index of CD4+ T cells cultured for 3 days in various types of media compositions (F). Culturing conditions (D, E, F): RPMI + 10% FCS TCR, RPMI + 10% FCS unstimulated, X-VIVO + 5% human serum TCR, X-VIVO + 5% human serum unstimulated, X-VIVO TCR, X-VIVO unstimulated. G0 = starting generation, G1 first generation, G2 second generation, etc.

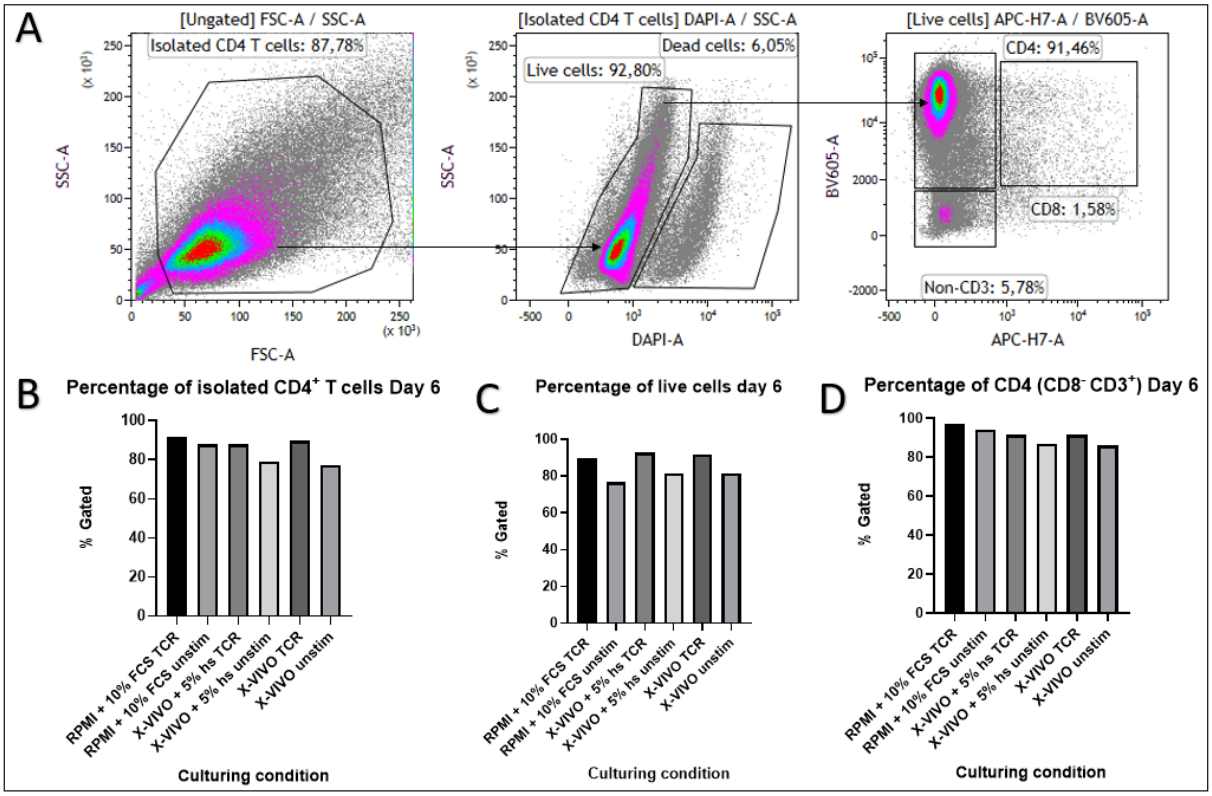

Fig 3.3.3 The effect of media composition on viability and purity of CD4⁺ T cell isolated from PBMCs isolated from fresh blood day 6. Representative gating strategy after 6 days of culturing CD4⁺ T cells isolated from PBMCs isolated from fresh blood (A). Percentage of isolated CD4⁺ T cells cultured for 6 days in various types of media compositions (B). Viability of CD4+ T cells cultured for 6 days in various types of media compositions (C). Purity of CD4+ T cells cultured for 6 days in various types of media compositions (D). Culturing conditions: RPMI + 10% FCS TCR, RPMI + 10% FCS unstimulated, X-VIVO + 5% human serum TCR, X-VIVO + 5% human serum unstimulated, X-VIVO TCR, X-VIVO unstimulated.

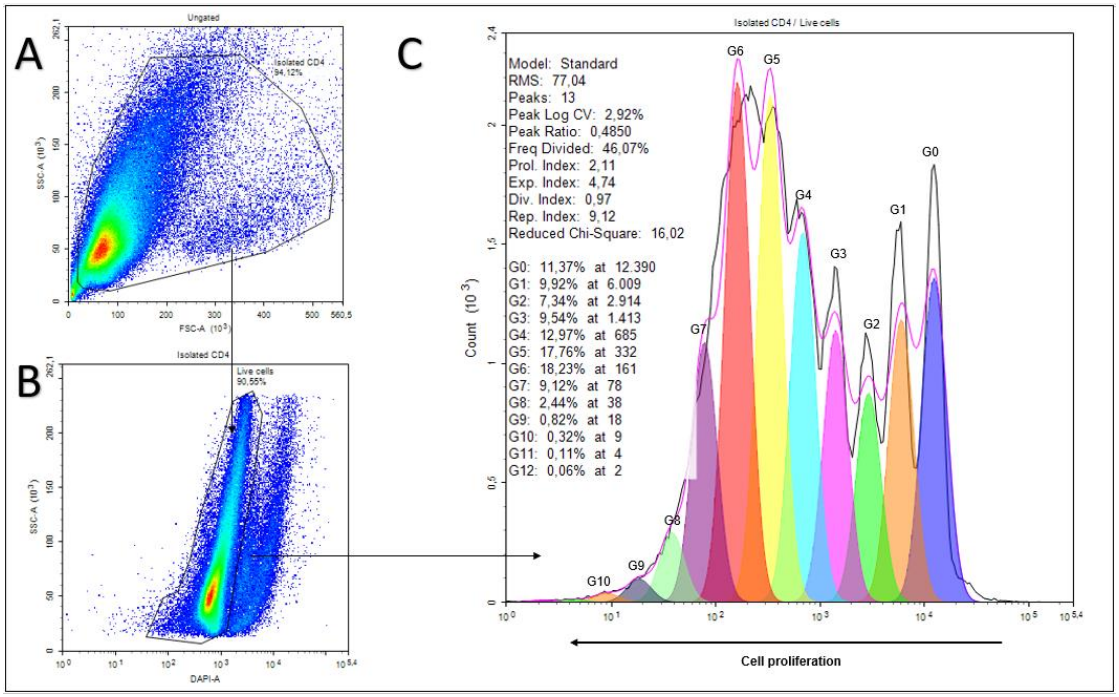

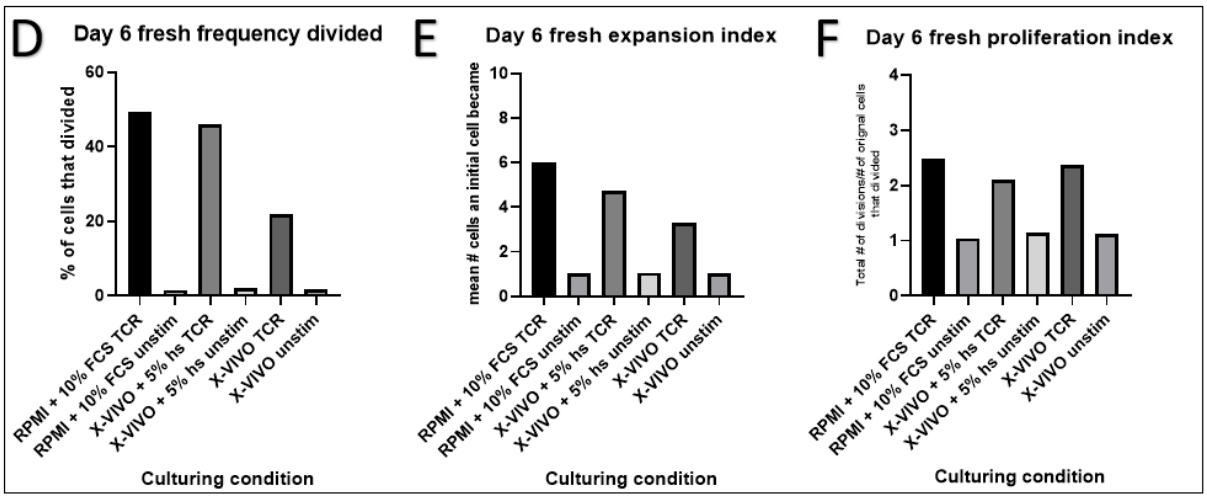

Fig. 3.3.4 The effect of media composition on cell proliferation of CD4⁺ T isolated from PBMCs isolated from fresh blood day 6. Representative gating strategy after 6 days of culturing CD4⁺ T cells isolated from PBMCs isolated from fresh blood (A, B, C). Frequency divided of CD4⁺ T cells cultured for 6 days in various types of media compositions (D). Expansion index of CD4⁺ T cells cultured for 6 days in various types of media compositions (E). Proliferation index of CD4⁺ T cells cultured for 6 days in various types of media compositions (F). Culturing conditions (D, E, F): RPMI + 10% FCS TCR, RPMI + 10% FCS unstimulated, X-VIVO + 5% human serum TCR, X-VIVO + 5% human serum unstimulated, X-VIVO TCR, X-VIVO unstimulated. G0 = starting generation, G1 first generation, G2 second generation, etc.

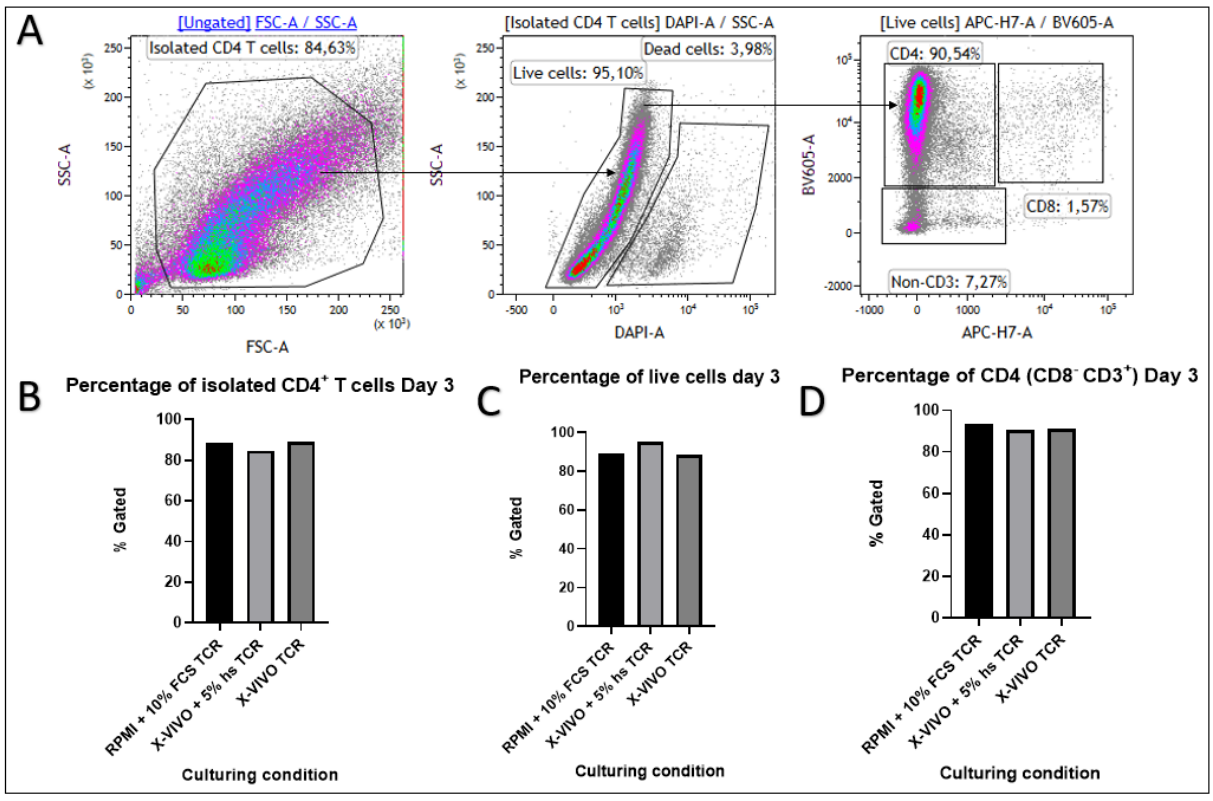

Fig 3.3.5 The effect of media composition on viability and purity of CD4⁺ T cell isolated from cryopreserved PBMCs day 3. Representative gating strategy after 3 days of culturing CD4⁺ T cells isolated from cryopreserved PBMCs (A). Percentage of isolated CD4⁺ T cultured for 3 days in various types of media compositions (B). Viability of CD4⁺ T cells cultured for 3 days in various types of media compositions (C). Purity of CD4⁺ T cells cultured for 3 days in various types of media compositions (D). Culturing conditions: RPMI + 10% FCS TCR, RPMI + 10% FCS unstimulated, X-VIVO + 5% human serum TCR, X-VIVO + 5% human serum unstimulated, X-VIVO TCR, X-VIVO unstimulated.

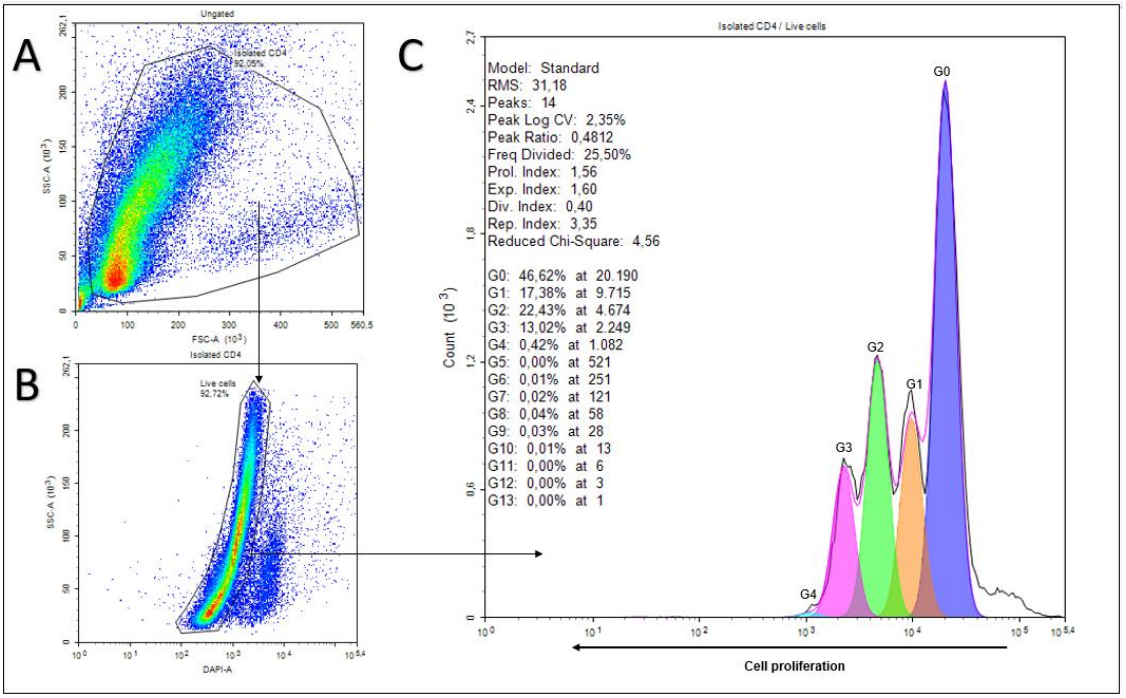

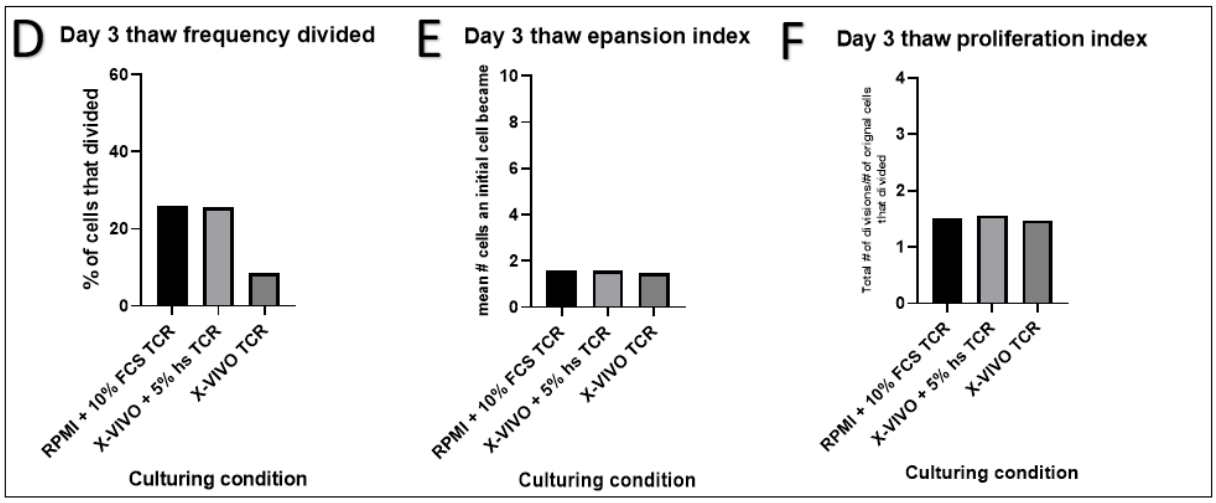

Fig 3.3.6 The effect of media composition on cell proliferation of CD4⁺ T isolated from cryopreserved PBMCs day 3. Representative gating strategy after 3 days of culturing CD4⁺ T cells isolated from cryopreserved PBMCs (A, B, C). Frequency divided of CD4⁺ T cells cultured for 3 days in various types of media compositions (D). Expansion index of CD4⁺ T cells cultured for 3 days in various types of media compositions (E). Proliferation index of CD4⁺ T cells cultured for 3 days in various types of media compositions (F). Culturing conditions (D, E, F): RPMI + 10% FCS TCR, RPMI + 10% FCS unstimulated, X-VIVO + 5% human serum TCR, X-VIVO + 5% human serum unstimulated, X-VIVO TCR, X-VIVO unstimulated. G0 = starting generation, G1 first generation, G2 second generation, etc.

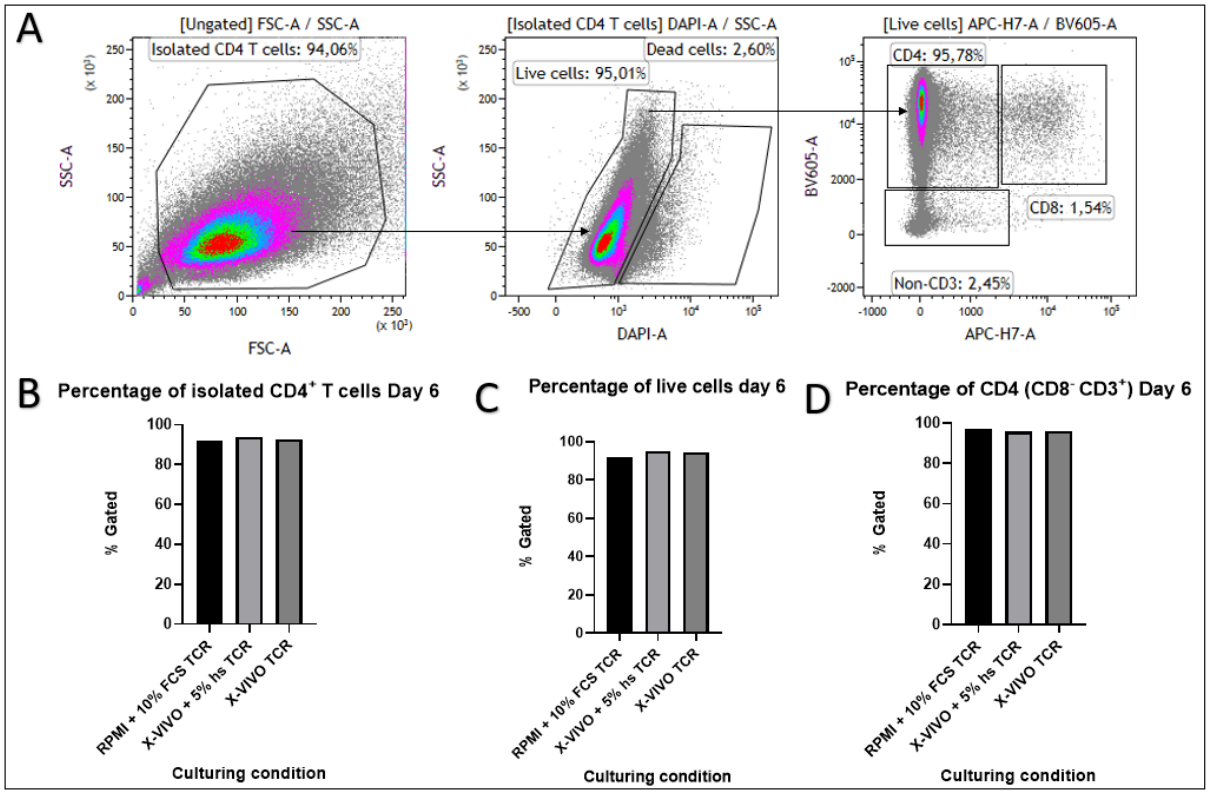

Fig. 3.3.7 The effect of media composition on viability and purity of CD4⁺ T cell isolated from cryopreserved PBMCs day 6. Representative gating strategy after 6 days of culturing CD4⁺ T cells isolated from cryopreserved PBMCs (A). Percentage of isolated CD4⁺ T cells cultured for 6 days in various types of media compositions (B). Viability of CD4⁺ T cells cultured for 6 days in various types of media compositions (C). Purity of CD4⁺ T cells cultured for 6 days in various types of media compositions (D). Culturing conditions: RPMI + 10% FCS TCR, RPMI + 10% FCS unstimulated, X-VIVO + 5% human serum TCR, X-VIVO + 5% human serum unstimulated, X-VIVO TCR, X-VIVO unstimulated.

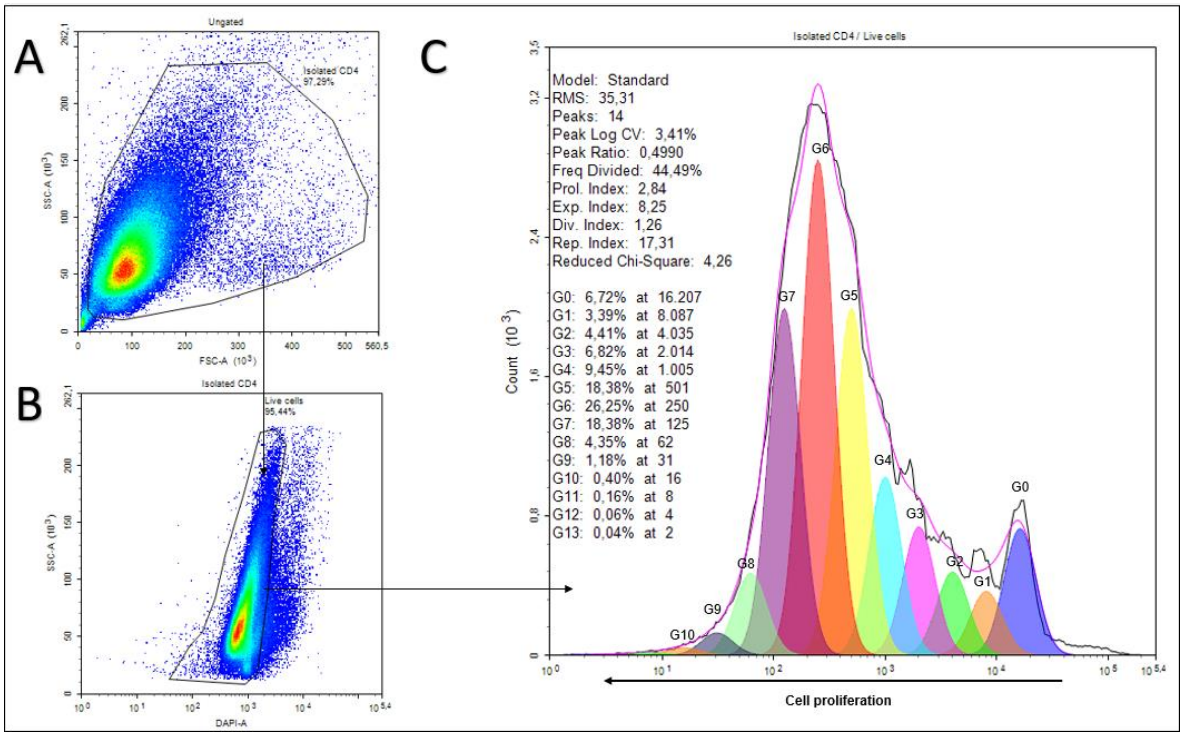

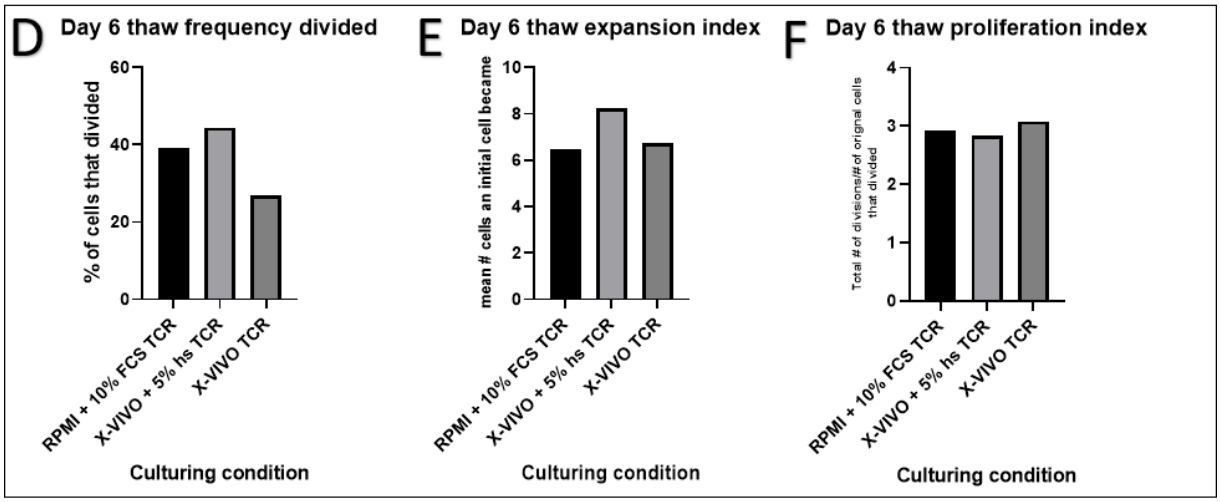

Fig 3.3.8 The effect of media composition on cell proliferation of CD4⁺ T isolated from cryopreserved PBMCs day 6. Representative gating strategy after 6 days of culturing CD4⁺ T cells isolated from cryopreserved PBMCs (A, B, C). Frequency divided of CD4⁺ T cells cultured for 6 days in various types of media compositions (D). Expansion index of CD4⁺ T cells cultured for 6 days in various types of media compositions (E). Proliferation index of CD4+ T cells cultured for 6 days in various types of media compositions (F). Culturing conditions (D, E, F): RPMI + 10% FCS TCR, RPMI + 10% FCS unstimulated, X-VIVO + 5% human serum TCR, X-VIVO + 5% human serum unstimulated, X-VIVO TCR, X-VIVO unstimulated. G0 = starting generation, G1 first generation, G2 second generation, etc.

3.4 Pim-1 kinase inhibitor (TCS PIM-1 1) and pan-Pim inhibitor (AZD1208) decrease CD4⁺ T cell proliferation without affecting cell viability and purity

To determine whether Pim kinase inhibitors interfere with the viability, purity and proliferation of CD4⁺ T cells, we investigated the effect of the Pim-1 kinase inhibitor TCS PIM-1 1 and the pan-Pim inhibitor AZD1208 on viability, purity and proliferative capacity of CD4⁺ T. In total 8 different conditions were investigated including RPMI + 10 % FCS unstimulated, RPMI +10 % FCS TCR DMSO, RPMI + 10% FCS TCR Pim-1i, RPMI + 10% FCS pan-Pim-i, X-VIVO + 5% HS unstimulated, X-VIVO + 5% HS TCR DMSO, X-VIVO TCR + 5% HS Pim-1i, X-VIVO + 5% HS pan-Pim-I (table 3.1)

Table 3.2 Culturing conditions media + inhibitors experiment

Medium	Serum	TCR stimuli	Condition
RPMI	10% FCS	Yes	DMSO
RPMI	10% FCS	Yes	PIM-1 inhibitor
RPMI	10% FCS	Yes	PanPim inhibitor
RPMI	10% FCS	No	N.A.
X-VIVO	5% HS	Yes	DMSO
X-VIVO	5% HS	Yes	PIM-1 inhibitor
X-VIVO	5% HS	Yes	PanPim inhibitor
X-VIVO	5% HS	No	N.A.

No major differences were found in viability and purity between the 4 conditions cultured in RPMI + 10% FCS. This was similar for the 4 conditions cultured in X-VIVO + 5% human serum. However, the 4 conditions cultured in X-VIVO + 5% human serum had a relative higher viability compared to the 4 conditions cultured in RPMI+ 10% FCS (fig 3.4.1C & D). After 3 days of culturing, we observed a decrease in cell proliferation of the $CD4^+$ T cells cultured with pim kinase inhibitors. The panPim inhibitor showed a stronger inhibitory effect on cell proliferation compared to the Pim-1 inhibitor. The frequency divided, expansion index and proliferation index were all decreased for the Pim inhibitor treated conditions compared to the DMSO treated condition in RPMI +10% FCS as well as in X-VIVO + 5% HS. The panPim inhibitor showed a stronger decrease on each of these cell proliferation statistics compared the Pim-1 inhibitor (fig 3.4.2D, E & F).

After 6 days of culturing, we observed no major differences regarding cell purity and viability between the 8 different conditions. However, we observed a clear decrease in viability for the unstimulated conditions compared to the TCR-stimulated conditions (fig 3.4.3C & D). Similar to day 3 we observed an overall decrease in cell proliferation for $CD4^+$ T cells treated with Pim kinase inhibitors when investigating the frequency divided, expansion index and proliferation index (fig 3.4.4D, E & F) One exception we observed was the relatively high frequency divided of the RPMI TCR Pim-i condition (fig 3.4.4D). Overall, the panPim inhibitor showed a stronger inhibitory effect on cell proliferation compared to the Pim-1 inhibitor reflected by all cell proliferation statistics except for the expansion index for cells in X-VIVO medium which was similar for both inhibitors.

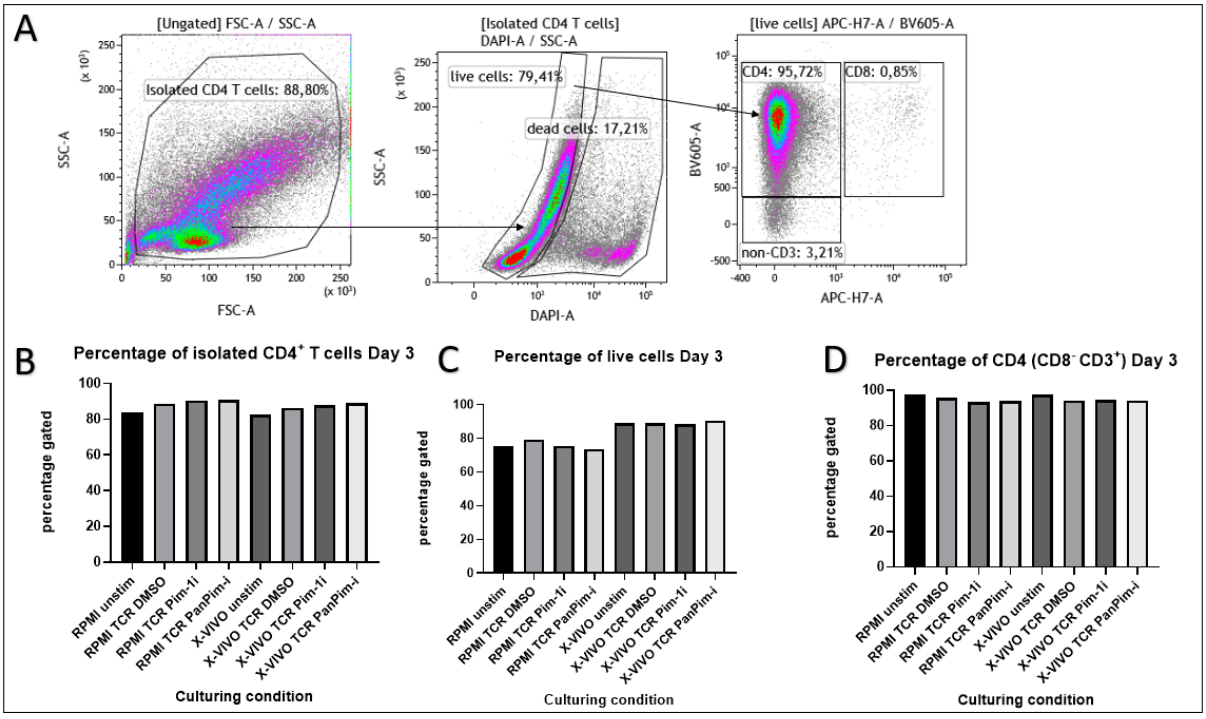

Fig 3.4.1 The effect of Pim-1 kinase inhibitor (TCS PIM-1 1) and pan-Pim inhibitor (AZD1208) on $CD4^+$ T cell viability and purity day 3. Representative gating strategy of the purity panel after 3 days of culturing (A). Percentage of isolated CD4+ T cell day 3 (B). Viability of the isolated $CD4^+$ T cells at day 3 (C). Purity of $CD4^+$ T cells at day 3. Culturing conditions: RPMI* unstimulated, RPMI TCR DMSO, RPMI TCR Pim-1i, RPMI pan-Pim-i, X-VIVO** unstimulated, X-VIVO TCR DMSO, X-VIVO TCR Pim-1i, X-VIVO pan-Pim-i. *RPMI was supplemented with 10 % FCS. **X-VIVO was supplemented with 5 % human serum.

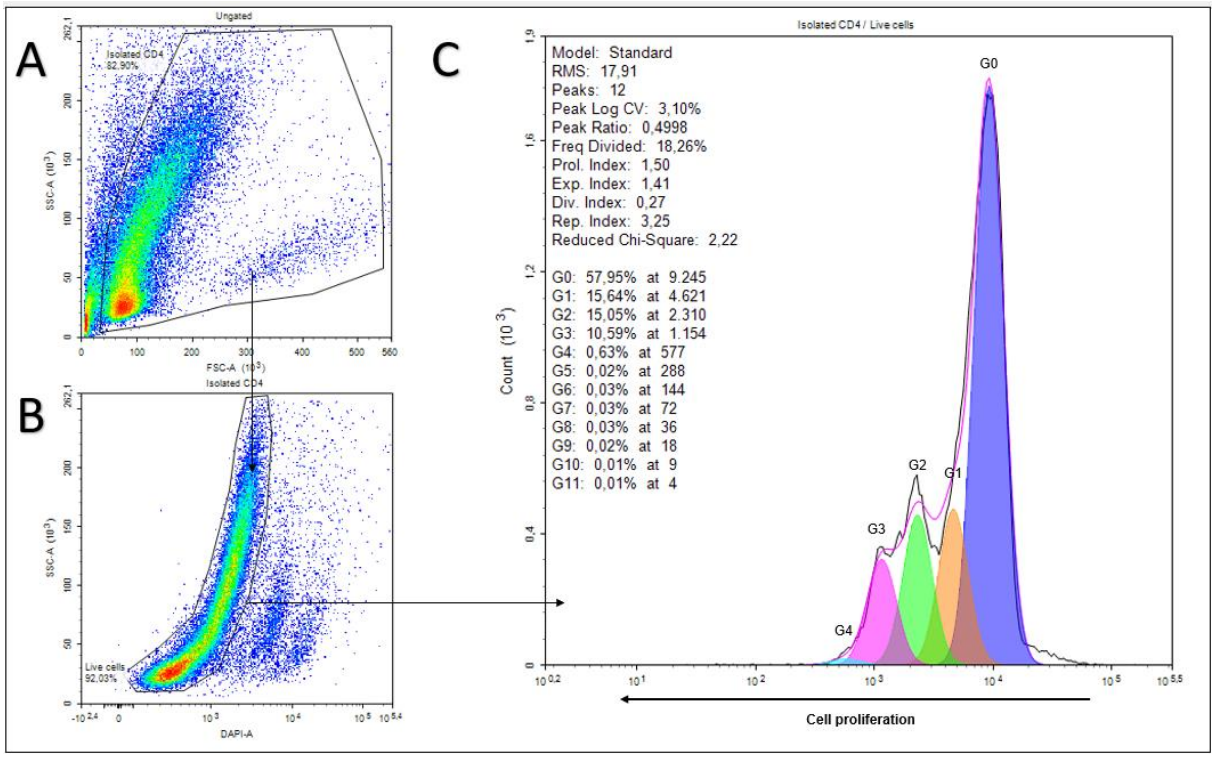

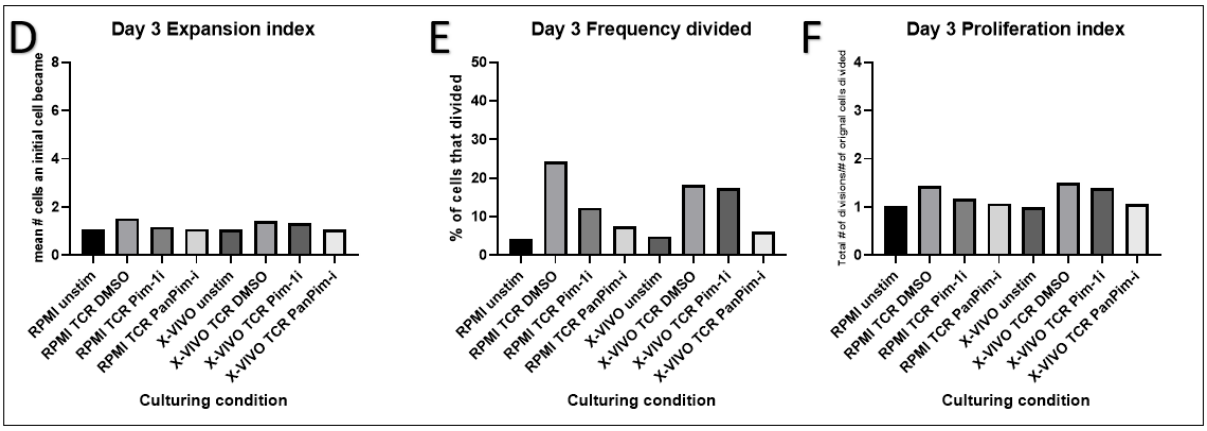

Fig 3.4.2 The effect of Pim-1 kinase inhibitor (TCS PIM-1 1) and pan-Pim inhibitor (AZD1208) on CD4⁺ T cell proliferation day 3. Representative gating strategy of the cell proliferation analysis after 3 days of culturing (A, B, C). Cell proliferation plot with proliferation fit statistics (C). Expansion index of the different culturing conditions at day 3 (D). Frequency divided of the different culturing conditions at day 3 (E). Proliferation index of the different culturing conditions at day 3 (F). Culturing conditions: RPMI* unstimulated, RPMI TCR DMSO, RPMI TCR Pim-1i, RPMI pan-Pim-i, X-VIVO** unstimulated, X-VIVO TCR DMSO, X-VIVO TCR Pim-1i, X-VIVO pan-Pim-i. G0 = starting generation, G1 first generation, G2 second generation, etc. *RPMI was supplemented with 10 % FCS. **X-VIVO was supplemented with 5 % human serum.

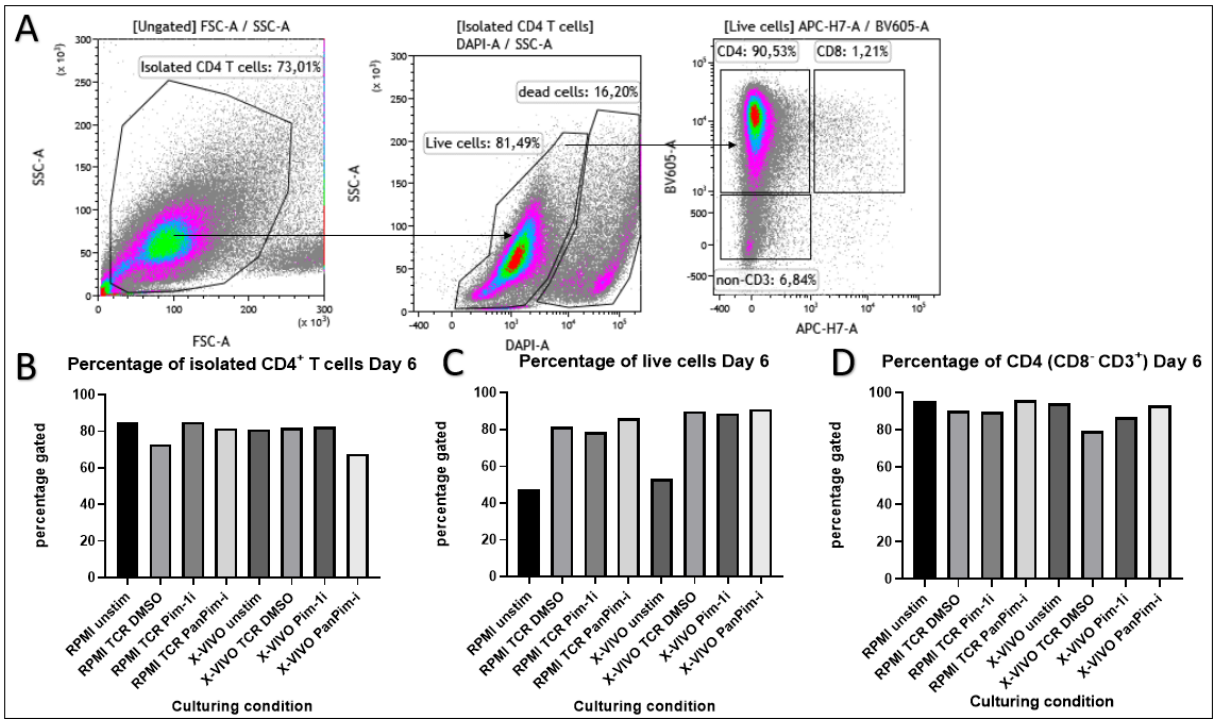

Fig 3.4.3 The effect of Pim-1 kinase inhibitor (TCS PIM-1 1) and pan-Pim inhibitor (AZD1208) on CD4⁺ T cell viability and purity day 6. Representative gating strategy of the purity panel after 6 days of culturing (A). Percentage of isolated CD4+ T cell day 6 (B). Viability of the isolated CD4⁺ T cells at day 6 (C). Purity of CD4⁺ T cells at day 6. Culturing conditions: RPMI* unstimulated, RPMI TCR DMSO, RPMI TCR Pim-1i, RPMI pan-Pim-i, X-VIVO** unstimulated, X-VIVO TCR DMSO, X-VIVO TCR Pim-1i, X-VIVO pan-Pim-i. *RPMI was supplemented with 10 % FCS. **X-VIVO was supplemented with 5 % human serum.

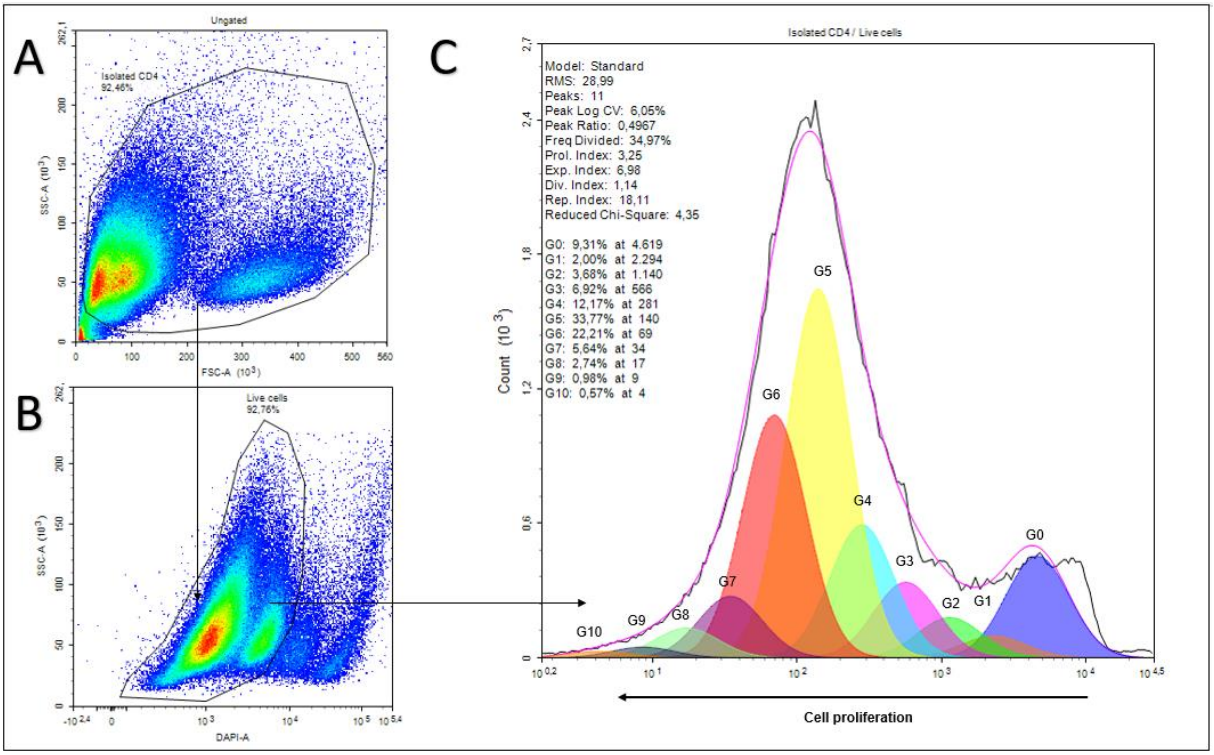

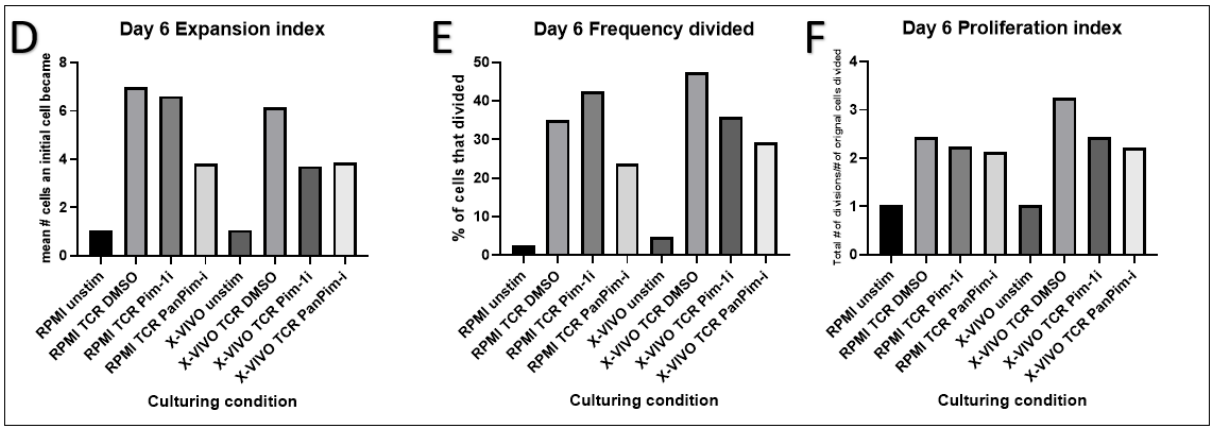

Fig 3.4.4 The effect of Pim-1 kinase inhibitor (TCS PIM-1 1) and pan-Pim inhibitor (AZD1208) on $CD4^+$ T cell proliferation day 6. Representative gating strategy of the cell proliferation analysis after 6 days of culturing (A, B, C). Cell proliferation plot with proliferation fit statistics (C). Expansion index of the different culturing conditions at day 6 (D). Frequency divided of the different culturing conditions at day 6 (E). Proliferation index of the different culturing conditions at day 6 (F). Culturing conditions: RPMI* unstimulated, RPMI TCR DMSO, RPMI TCR Pim-1i, RPMI pan-Pim-i, X-VIVO** unstimulated, X-VIVO TCR DMSO, X-VIVO TCR Pim-1i, X-VIVO pan-Pim-i. G0 = starting generation, G1 first generation, G2 second generation, etc. *RPMI was supplemented with 10 % FCS. **X-VIVO was supplemented with 5 % human serum.

4. Discussion

This study aimed to optimize the conditions for the *in vitro* characterization of $CD4^+$ T cells proliferation and activation to study the effects of inhibition of Pim kinases on $CD4^+$ T cells from GPA patients. The rationale for studying Pim-1 kinase comes from previous studies showing an upregulation of Pim-1 kinase in $CD4^+$ T cell cells of early RA [48] and recent observations from our group demonstrating increased expression of Pim-1 mRNA in all $CD4^+$ T cell subsets in active GPA patients. In GPA, Tem Pim-1 mRNA levels and mRNA levels of its transcription factor STAT3 were also found to be increased in a subgroup of GPA remission patients suggesting that in clinical remission these patients' T cells are not quiescent. These observations indicate that the STAT3/PIM1 signaling pathway is activated in T cells from GPA patients and may be a target for treatment similar to what has been proposed for early arthritis by Maney et al. These investigators demonstrated that Pim kinase inhibition with either the pan-Pim inhibitor AZD1208 or the Pim-1 inhibitor TCS-PIM-1 1, decreased production of the Th1 specific cytokine IFN-y and the Th17 specific cytokine IL-17A. Moreover, Pim kinase inhibition decreased the proliferative capacity of the $CD4^+$ T cells and decreased the activation marker CD25, while not interfering with the viability of the cells. Lastly, they found a significant increase in the frequency of FoxP3+ cells and Tregs ($CD25^{high}FoxP3^+$) [48]. Since GPA is characterized by an expansion of Tem cells in conjunction with a diminished function of Tregs, inhibiting Pim kinases may be of benefit for GPA patients by normalizing the T cell balance. As a first step to study the effect of PIM kinase inhibition on $CD4^+$ T cells in GPA, this study primarily focused on optimizing the conditions for the *in vitro* activation and proliferation of $CD4^+$ T cells.

The first important objective was optimizing the isolation of $CD4^+$ T cells from PBMCs. We first checked the percentage of $CD4^+$ T in PBMCs and determined that in the cryopreserved PBMCs the percentage of $CD4^+$ T cells is 45.22%. MiltenyiBiotec, a well-established biotechnology company, reports that in isolated PBMCs, the percentage of $CD4^+$ T cells ranges from 25-60% [50] although it has been reported that the percentage of $CD4^+$ T cells in PBMCs decreases after cryopreservation [51, 52, 53]. The percentage reported in this study is within the range reported in the literature.

An important requirement for obtaining reliable results is the purity of the isolated fraction of $CD4^+$ T cells. Here we used negative selection to isolate $CD4^+$ T cells. The kit used for CD4+ T cell isolation in this study makes use of RapidSphere beads that are labelled with antibodies that bind to cell surface molecules of the unwanted cells. The cell type of interest remains untouched and can be collected for further use [54]. Stemcell Technologies, the manufacturers of the EasySep™ Human $CD4^+$ T Cell Isolation kit used in this study, report a purity ($CD3^+CD4^+$) of the isolated fraction of 94.8 ± 2.3%. In this study, a purity was obtained of ± 97%, which is on the upper side of the range reported by StemCell technologies. Next to negative selection, there is also positive selection. Positive selection works by selecting directly the cells of interest by targeting a cell surface marker expressed by the cells of interest with a ligand or antibody that is linked to a magnetic particle. Advantages of positive selection are that the purity of the procedure is higher compared to negative selection. However, a

disadvantage is that the isolated cell fraction often is bound by antibodies and magnetic particles. When the downstream application of the cells of interest is FACS as in this study, the antibodies are still bound to the isolated cell fraction from the isolation procedure could interfere with staining of specific cell surface makers for FACS. Negative selection does not label the cells of interest with antibodies and the procedure is also much quicker compared to the positive selection of target cells [55]. Therefore, negative selection is the preferred method for enrichment of target cells, in our case $CD4^+$ T cells.

We next determined which type of medium would be optimal for culturing in terms of cell viability, purity and cell proliferation of the $CD4^+$ T cells. We found that both RPMI supplemented with 10% FCS as X-VIVO supplemented with 5% HS showed relatively better cell proliferation compared to X-VIVO non-supplemented based upon the frequency divided, expansion index and proliferation index. However, differences were minimal. $CD4^+$ T cells isolated from fresh blood and those from cryopreserved PBMCs showed similar proliferation capacity in RPMI + 10% FCS and X-VIVO + 5% HS. However, not only cellular proliferation should determine what medium to use. In this study, X-VIVO supplemented with 5% HS has been chosen for the final experiment. X-VIVO is a proprietary medium of which the exact formulation is not known. However, it is described as an improved medium formulation with more defined serum components, hence it is called a serum free medium [56]. The most commonly used medium for T cell culturing in vitro is RPMI 1640 supplemented with 10% FBS. This medium was optimized mid-20^{th} century to favor the growth of many cell lines. Nowadays, there is much more known about the metabolic changes during differentiation and proliferation of T cells [57]. For instance, naïve lymphocytes mainly rely on oxidative phosphorylation to increase their maximum production of ATP [58]. However, when lymphocytes are activated, start to proliferate and become effector cells, the metabolism switches to glycolysis for the production of biosynthetic intermediates that support the activation, growth and effector functions of the cell. Within effector subsets, there are also differences in metabolism. Th1, Th2 and Th17 cells are more glycolytic compared to Tregs that rely more on fatty acid oxidation [59]. Lastly, when effector cells transition to memory cells, their metabolism switches again now relying mainly on fatty acid oxidation [59, 60]. Moreover, their mitochondrial mass increases as well as their respiratory capacity. This allows them to transition fast into effector cells upon restimulation and carry out their effector function [59, 61]. Many media currently used do not consider these advances in knowledge, which can be seen in for instance adoptive T cell therapy where T cells are expanded in RPMI 1640, AIM-V or X-VIVO supplemented with 5% HS and there is no general consensus on which medium is the best for expansion of human T cells for adoptive T cell therapy [62]. However, recently a study found that T cells for adoptive T cell therapy expanded in serum free media such as X-VIVO have more durable anti-tumor responses. They also found that T cells expansion in X-VIVO was similar between T cells cultured with HS compared to T cells cultured without HS. For RPMI, serum was needed to expand T cells in vitro. However, T cells expanded X-VIVO without serum showed an earlier decline in the population doubling rate compared to T cells expanded in X-VIVO with serum [62]. Moreover, when expanding $CD4^+$ naïve T cells in X-VIVO

without serum, effector T cells did not proliferate well [62]. This supports the use X-VIVO with HS for our experimental protocol.

Furthermore, metabolism and nutrient uptake by T cells has been shown to be dependent on the media composition. When switching T cells to a different medium, they can adopt their metabolism to this medium. However, their function does not change by switching medium [56]. When culturing T cells in 5 different media compositions the proportions of T naïve, T central memory, T effector and T effector memory cells, differed between 5 media compositions studied [56]. So, when studying a particular subset, for example Tem cells, one might consider expanding $CD4^+$ T cells in REP medium, since this medium shows the highest percentage of $CD4^+$ Tem cells after 12 days of expanding. Next to differentiation also activation is influenced by the expansion condition. The percentage of $CD25^+$ T cells was the highest for $CD4^+$ T cells and $CD8^+$ T cells cultured in human plasma-like medium compared to the 4 other media compositions [56]. Moreover, when comparing lymphocytes cultured in RMPI 1640 with those cultured in human plasma-like medium (HPLM) (both supplemented with dialyzed FBS), it was found that primary human T cells expanded in HPLM had different transcriptional responses and improved activation upon antigen stimulation compared to primary human T cells cultured in RPMI. Many of the most differentially expressed genes for T cells expanded in HPLM were genes that encode for enzymes that are rate-limiting in amino acid metabolism [57]. HPML is a medium that has physiological concentrations of amino acids hormones and glucose. RPMI on the other hand relies on FBS to supply these nutrients, however they are often present in non-physiological concentrations present [57, 59]. In vitro expansion of T cells in a physiological medium such as HPML might better resemble the biological functioning, differentiation and activation of T cells in vivo. However, media like this may need the addition of human serum to induce and sustain proper T cell expansion [57].

Additionally, the ratio of $CD4^+$ T cells to $CD8^+$ T cells is influenced by the medium. For example, rapid expansion protocol (REP) medium, which is a 1:1 mix of RMPI 1640 and AIM-V supplemented with 5% HS has an increased percentage of $CD4^+$ T cells and a decreased percentage of $CD8^+$ T cells [56]. Moreover, after 12 days of culturing the REP medium had the highest yield of T cells compared to 4 other expansion conditions [56]. This indicates that the expansion condition next to the differentiation and activation of T cells also skews the proliferation of T cells. Considering that our studies are focused on the $CD4^+$ T cells, switching to this medium might result in a higher proportion of $CD4^+$ T cells for downstream analyses. This could be of benefit as it may reduce the amount of blood that has to be taken from patients.

Lastly, in preliminary experiments we found that Pim kinase inhibition reduced cell proliferation when examining the frequency divided, expansion index and proliferation index. Viability on the other hand remained the same between the culturing conditions. The Pim-1 kinase inhibitor (TCS PIM-1 1) seems to decrease cell proliferation of the cultured $CD4^+$ T cells, which can already be seen after 3 days of culturing. The same holds true for the pan-Pim inhibitor (AZD1208) that showed an even stronger inhibitory effect on the proliferation of $CD4^+$ T cells compared to the Pim-1 kinase inhibitor (TCS PIM-1 1). These effects seem to be

persistent across different healthy controls (data not shown) whereas the pattern observed is in accordance with that observed by Maney et al. [48].

5. Conclusions

In vitro activation studies of $CD4^+$ T cells is dependent on a large numbers of variables that can impact the results, such as the isolation of $CD4^+$ T cells, the concentration of TCR stimuli and the media composition for culturing the cells. It is of uttermost importance that researchers keep in mind these variables to interpret the results in the most accurate way. Here, we have optimized all these variables for studying the effect of PIM inhibition of $CD4^+$ T cell function in GPA, with our most important conclusions listed below.

- Fresh PBMCs give a higher yield of $CD4^+$ T cells compared to cryopreserved PBMCs, without affecting the viability and purity of the isolated cell fraction.
- The optimal concentration of TCR stimuli was estimated at 0.5 µg/ml plate-bound anti-CD3 and 1 µg/ml soluble anti CD28/49d
- RPMI + 10% FCS and X-VIVO + 5% HS show similar viability, purity and cell proliferation of $CD4^+$ T cells after 3 and 6 days of culturing. X-VIVO shows similar viability and purity as well, however cell proliferation is affected when examining the frequency divided.
- PIM kinase inhibitors decrease cell proliferation without affecting the viability and purity compared to the DMSO control
- The pan-PIM inhibitor (AZD1208) shows a stronger effect on the cell proliferation of $CD4^+$ T cells compared to the PIM-1 inhibitors (TCS 1)
- Cell proliferation data should be interpreted with caution as various software packages give the same name to distinct cell proliferation statistics

References

1. Kitching, A. R., Anders, H. J., Basu, N., Brouwer, E., Gordon, J., Jayne, D. R., Kullman, J., Lyons, P. A., Merkel, P. A., Savage, C. O. S., Specks, U., & Kain, R. (2020). ANCA-associated vasculitis. Nature Reviews Disease Primers, 6(1). https://doi.org/10.1038/s41572-020-0204-y

2. Diseases and Conditions Vasculitis. (n.d.). Rheumatology.org. Retrieved December 21, 2021, from https://www.rheumatology.org/I-Am-A/Patient-Caregiver/Diseases Conditions/Vasculitis

3. von Borstel, A., Sanders, J. S., Rutgers, A., Stegeman, C. A., Heeringa, P., & Abdulahad, W. H. (2018). Cellular immune regulation in the pathogenesis of ANCA-associated vasculitides. Autoimmunity Reviews, 17(4), 413–421. https://doi.org/10.1016/j.autrev.2017.12.002

4. Houben, E., Bax, W. A., van Dam, B., Slieker, W. A., Verhave, G., Frerichs, F. C., van Eijk, I. C., Boersma, W. G., de Kuyper, G. T., & Penne, E. L. (2016). Diagnosing ANCA-associated vasculitis in ANCA positive patients. Medicine, 95(40), e5096. https://doi.org/10.1097/md.0000000000005096

5. Moog, P., & Thuermel, K. (2015). Spotlight on rituximab in the treatment of antineutrophil cytoplasmic antibody-associated vasculitis: current perspectives. Therapeutics and clinical risk management, 11, 1749–1758. https://doi.org/10.2147/TCRM.S79080

6. King, C., Druce, K. L., Nightingale, P., Kay, E., Basu, N., Salama, A. D., & Harper, L. (2021). Predicting relapse in anti-neutrophil cytoplasmic antibody-associated vasculitis: a Systematic review and meta-analysis. Rheumatology Advances in Practice, 5(3). https://doi.org/10.1093/rap/rkab018

7. Salama, A. D. (2020). Relapse in Anti-Neutrophil Cytoplasm Antibody (ANCA)–Associated Vasculitis. Kidney International Reports, 5(1), 7–12. https://doi.org/10.1016/j.ekir.2019.10.005

8. Hirayama, K. (2020). The pathogenesis of antineutrophil cytoplasmic antibody-associated vasculitis : Breakage or failure of self-immune tolerance mechanisms. The Journal of Tokyo Medical University , 78（2）: 130- 140

9. Cartin-Ceba, R., Peikert, T., & Specks, U. (2012). Pathogenesis of ANCA-Associated Vasculitis. Current Rheumatology Reports, 14(6), 481–493. https://doi.org/10.1007/s11926-012-0286-y

10. Alberola-Ila, J., Hogquist, K. A., Swan, K. A., Bevan, M. J., & Perlmutter, R. M. (1996). Positive and negative selection invoke distinct signaling pathways. Journal of Experimental Medicine, 184(1), 9–18. https://doi.org/10.1084/jem.184.1.9

11. Brilland, B., Garnier, A. S., Chevailler, A., Jeannin, P., Subra, J. F., & Augusto, J. F. (2020). Complement alternative pathway in ANCA-associated vasculitis: Two decades from bench to bedside. Autoimmunity Reviews, 19(1), 102424. https://doi.org/10.1016/j.autrev.2019.102424

12. Jarrot, P. A., & Kaplanski, G. (2016). Pathogenesis of ANCA-associated vasculitis: An update. Autoimmunity Reviews, 15(7), 704–713. https://doi.org/10.1016/j.autrev.2016.03.007

13. Vorobjeva, N. V., & Chernyak, B. V. (2020). NETosis: Molecular Mechanisms, Role in Physiology and Pathology. Biochemistry (Moscow), 85(10), 1178–1190. https://doi.org/10.1134/s0006297920100065

14. Sangaletti, S., Tripodo, C., Chiodoni, C., Guarnotta, C., Cappetti, B., Casalini, P., Piconese, S., Parenza, M., Guiducci, C., Vitali, C., & Colombo, M. P. (2012). Neutrophil extracellular traps mediate transfer of cytoplasmic neutrophil antigens to myeloid dendritic cells toward ANCA induction and associated autoimmunity. Blood, 120(15), 3007–3018. https://doi.org/10.1182/blood-2012-03-416156

15. Lintermans, L. L., Rutgers, A., Stegeman, C. A., Heeringa, P., & Abdulahad, W. H. (2017). Chemokine receptor co-expression reveals aberrantly distributed TH effector memory cells in GPA patients. Arthritis Research & Therapy, 19(1). https://doi.org/10.1186/s13075-017-1343-8

16. Schmitt, W. H., Hagen, E. C., Neumann, I., Nowack, R., Flores-Suárez, L. F., Van der Woude, F. J., & For The European Vasculitis Study Group. (2004). Treatment of refractory Wegener's granulomatosis with antithymocyte globulin (ATG): An open study in 15 patients. Kidney International, 65(4), 1440–1448. https://doi.org/10.1111/j.1523-1755.2004.00534.x

17. Ruth, A. J., Kitching, A. R., Kwan, R. Y., Odobasic, D., Ooi, J. D., Timoshanko, J. R., Hickey, M. J., & Holdsworth, S. R. (2006). Anti-Neutrophil Cytoplasmic Antibodies and Effector CD4+Cells Play Nonredundant Roles in Anti-Myeloperoxidase Crescentic Glomerulonephritis. Journal of the American Society of Nephrology, 17(7), 1940–1949. https://doi.org/10.1681/asn.2006020108

18. Wilde, B., Thewissen, M., Damoiseaux, J., van Paassen, P., Witzke, O., & Tervaert, J. W. (2010). T cells in ANCA-associated vasculitis: what can we learn from lesional versus circulating T cells? Arthritis Research & Therapy, 12(1), 204. https://doi.org/10.1186/ar2923

19. ABDULAHAD, W. H., STEGEMAN, C. A., & KALLENBERG, C. G. (2009). Review article: The role of CD4+T cells in ANCA-associated systemic vasculitis. Nephrology, 14(1), 26–32. https://doi.org/10.1111/j.1440-1797.2008.01069.x

20. Martinez Valenzuela, L., Bordignon Draibe, J., Fulladosa Oliveras, X., Bestard Matamoros, O., Cruzado Garrit, J. M., & Torras Ambrós, J. (2019). T-lymphocyte in ANCA-associated vasculitis: what do we know? A pathophysiological and therapeutic approach. Clinical Kidney Journal, 12(4), 503–511. https://doi.org/10.1093/ckj/sfz029

21. Lilliebladh, S., Johansson, S., Pettersson, S., Ohlsson, S., & Hellmark, T. (2018). Phenotypic Characterization of Circulating CD4+ T Cells in ANCA-Associated Vasculitis. Journal of Immunology Research, 2018, 1–12. https://doi.org/10.1155/2018/6984563

22. Raphael, I., Nalawade, S., Eagar, T. N., & Forsthuber, T. G. (2015). T cell subsets and their signature cytokines in autoimmune and inflammatory diseases. Cytokine, 74(1), 5–17. https://doi.org/10.1016/j.cyto.2014.09.011

23. Aarvak, T., Chabaud, M., Thoen, J., Miossec, P., & Natvig, J. B. (2000). Changes in the Th1 or Th2 cytokine dominance in the synovium of rheumatoid arthritis (RA): a kinetic study of the Th subsets in one unusual RA patient. Rheumatology, 39(5), 513–522. https://doi.org/10.1093/rheumatology/39.5.513

24. Abdulahad, W. H., Stegeman, C. A., Limburg, P. C., & Kallenberg, C. G. M. (2008). Skewed distribution of Th17 lymphocytes in patients with Wegener's granulomatosis in remission. Arthritis & Rheumatism, 58(7), 2196–2205. https://doi.org/10.1002/art.23557

25. Abdulahad, W. H., van der Geld, Y. M., Stegeman, C. A., & Kallenberg, C. G. (2006). Persistent expansion of CD4+ effector memory T cells in Wegener's granulomatosis. Kidney international, 70(5), 938–947. https://doi.org/10.1038/sj.ki.5001670

26. Popa, E. R., Franssen, C. F. M., Limburg, P. C., Huitema, M. G., Kallenberg, C. G. M., & Cohen Tervaert, J. W. (2002). In vitro cytokine production and proliferation of T cells from patients with anti-proteinase 3- and antimyeloperoxidase-associated vasculitis, in response to proteinase 3 and myeloperoxidase. Arthritis & Rheumatism, 46(7), 1894–1904. https://doi.org/10.1002/art.10384

27. Szczeklik, W., Jakieła, B., Wawrzycka-Adamczyk, K., Sanak, M., Hubalewska-Mazgaj, M., Padjas, A., Surmiak, M., Szczeklik, K., Sznajd, J., & Musiał, J. (2017). Skewing toward Treg and Th2 responses is a characteristic feature of sustained remission in ANCA-positive granulomatosis with polyangiitis. European Journal of Immunology, 47(4), 724–733. https://doi.org/10.1002/eji.201646810

28. King, C., Druce, K. L., Nightingale, P., Kay, E., Basu, N., Salama, A. D., & Harper, L. (2021). Predicting relapse in anti-neutrophil cytoplasmic antibody-associated vasculitis: a Systematic review and meta-analysis. Rheumatology advances in practice, 5(3), rkab018. https://doi.org/10.1093/rap/rkab018

29. Yasuda, K., Takeuchi, Y., & Hirota, K. (2019). The pathogenicity of Th17 cells in autoimmune diseases. Seminars in immunopathology, 41(3), 283–297. https://doi.org/10.1007/s00281-019-00733-8

30. Wilde, B., Thewissen, M., Damoiseaux, J., Hilhorst, M., van Paassen, P., Witzke, O., & Cohen Tervaert, J. (2012). Th17 expansion in granulomatosis with polyangiitis (Wegener's): the role of disease activity, immune regulation and therapy. Arthritis Research & Therapy, 14(5), R227. https://doi.org/10.1186/ar4066

31. Pelletier, M., Maggi, L., Micheletti, A., Lazzeri, E., Tamassia, N., Costantini, C., Cosmi, L., Lunardi, C., Annunziato, F., Romagnani, S., & Cassatella, M. A. (2010). Evidence for a cross-talk between human neutrophils and Th17 cells. Blood, 115(2), 335–343. https://doi.org/10.1182/blood-2009-04-216085

32. Robert, M., Miossec, P., & Hot, A. (2022). The Th17 Pathway in Vascular Inflammation: Culprit or Consort? Frontiers in Immunology, 13. https://doi.org/10.3389/fimmu.2022.888763

33. Wu, X., Tian, J., & Wang, S. (2018). Insight Into Non-Pathogenic Th17 Cells in Autoimmune Diseases. Frontiers in Immunology, 9. https://doi.org/10.3389/fimmu.2018.01112

34. Nogueira, E., Hamour, S., Sawant, D., Henderson, S., Mansfield, N., Chavele, K. M., Pusey, C. D., & Salama, A. D. (2010). Serum IL-17 and IL-23 levels and autoantigen-specific Th17 cells are elevated in patients with ANCA-associated vasculitis. Nephrology Dialysis Transplantation, 25(7), 2209–2217. https://doi.org/10.1093/ndt/gfp783

35. Free, M. E., Bunch, D. O., McGregor, J. A., Jones, B. E., Berg, E. A., Hogan, S. L., Hu, Y., Preston, G. A., Jennette, J. C., Falk, R. J., & Su, M. A. (2013). Patients With Antineutrophil Cytoplasmic Antibody-Associated Vasculitis Have Defective Treg Cell Function Exacerbated by the Presence of a Suppression-Resistant Effector Cell Population. Arthritis & Rheumatism, 65(7), 1922–1933. https://doi.org/10.1002/art.37959

36. Abdulahad, W. H., Kallenberg, C. G. M., Limburg, P. C., & Stegeman, C. A. (2009). Urinary CD4+ effector memory T cells reflect renal disease activity in antineutrophil cytoplasmic antibody-associated vasculitis. Arthritis & Rheumatism, 60(9), 2830–2838. https://doi.org/10.1002/art.24747

37. Takatori, H., Kawashima, H., Matsuki, A., Meguro, K., Tanaka, S., Iwamoto, T., Sanayama, Y., Nishikawa, N., Tamachi, T., Ikeda, K., Suto, A., Suzuki, K., Kagami, S. I., Hirose, K., Kubo, M., Hori, S., & Nakajima, H. (2015). Helios Enhances Treg Cell Function in Cooperation With FoxP3. Arthritis & Rheumatology, 67(6), 1491–1502. https://doi.org/10.1002/art.39091

38. Thornton, A. M., & Shevach, E. M. (2019). Helios: still behind the clouds. Immunology, 158(3), 161–170. https://doi.org/10.1111/imm.13115

39. Abdulahad, W. H., Lepse, N., Stegeman, C. A., Huitema, M. G., Doornbos-van Der Meer, B., Tadema, H., Rutgers, A., Limburg, P. C., Kallenberg, C. G., & Heeringa, P. (2013). Increased frequency of circulating IL-21 producing Th-cells in patients with granulomatosis with polyangiitis (GPA). Arthritis Research & Therapy, 15(3), R70. https://doi.org/10.1186/ar4247

40. Xu, Y., Xu, H., Zhen, Y., Sang, X., Wu, H., Hu, C., Ma, Z., Yu, M., & Yi, H. (2019). Imbalance of Circulatory T Follicular Helper and T Follicular Regulatory Cells in Patients with ANCA-Associated Vasculitis. Mediators of Inflammation, 2019, 1–9. https://doi.org/10.1155/2019/8421479

41. Choi, J., Diao, H., Faliti, C. E., Truong, J., Rossi, M., Bélanger, S., Yu, B., Goldrath, A. W., Pipkin, M. E., & Crotty, S. (2020). Bcl-6 is the nexus transcription factor of T follicular helper cells via repressor-of-repressor circuits. Nature Immunology, 21(7), 777–789. https://doi.org/10.1038/s41590-020-0706-5

42. Liu, Z., Han, M., Ding, K., & Fu, R. (2020). The role of Pim kinase in immunomodulation. American journal of cancer research, 10(12), 4085–4097.

43. Warfel, N. A., & Kraft, A. S. (2015). PIM kinase (and Akt) biology and signaling in tumors. Pharmacology & Therapeutics, 151, 41–49. https://doi.org/10.1016/j.pharmthera.2015.03.001

44. Jackson, L. J., Pheneger, J. A., Pheneger, T. J., Davis, G., Wright, A. D., Robinson, J. E., Allen, S., Munson, M. C., & Carter, L. L. (2012). The role of PIM kinases in human and mouse CD4+ T cell activation and inflammatory bowel disease. Cellular Immunology, 272(2), 200–213. https://doi.org/10.1016/j.cellimm.2011.10.011

45. Li, Z., Lin, F., Zhuo, C., Deng, G., Chen, Z., Yin, S., Gao, Z., Piccioni, M., Tsun, A., Cai, S., Zheng, S. G., Zhang, Y., & Li, B. (2014). PIM1 Kinase Phosphorylates the Human Transcription Factor FOXP3 at Serine 422 to Negatively Regulate Its Activity under Inflammation. Journal of Biological Chemistry, 289(39), 26872–26881. https://doi.org/10.1074/jbc.m114.586651

46. Wang, M., Okamoto, M., Domenico, J., Han, J., Ashino, S., Shin, Y. S., & Gelfand, E. W. (2012). Inhibition of Pim1 kinase prevents peanut allergy by enhancing Runx3 expression and suppressing TH2 and TH17 T-cell differentiation. Journal of Allergy and Clinical Immunology, 130(4), 932–944.e12. https://doi.org/10.1016/j.jaci.2012.07.032

47. Tahvanainen, J., Kyläniemi, M. K., Kanduri, K., Gupta, B., Lähteenmäki, H., Kallonen, T., Rajavuori, A., Rasool, O., Koskinen, P. J., Rao, K. V., Lähdesmäki, H., & Lahesmaa, R. (2013). Proviral Integration Site for Moloney Murine Leukemia Virus (PIM) Kinases Promote Human T Helper 1 Cell Differentiation. Journal of Biological Chemistry, 288(5), 3048–3058. https://doi.org/10.1074/jbc.m112.361709

48. Maney, N. J., Lemos, H., Barron-Millar, B., Carey, C., Herron, I., Anderson, A. E., Mellor, A. L., Isaacs, J. D., & Pratt, A. G. (2021). Pim Kinases as Therapeutic Targets in Early Rheumatoid Arthritis. Arthritis & Rheumatology, 73(10), 1820–1830. https://doi.org/10.1002/art.41744

49. Roederer, M. (2011). Interpretation of cellular proliferation data: Avoid the panglossian. *Cytometry Part A*, *79A*(2), 95–101. https://doi.org/10.1002/cyto.a.21010

50. *Peripheral Blood | Whole blood | Handbook | Miltenyi Biotec | Nederland*. (z.d.). Miltenyibiotec. Geraadpleegd op 1 juli 2022, van https://www.miltenyibiotec.com/NL-en/resources/macs-handbook/human-cells-and-organs/human-cell-sources/blood-human.html?countryRedirected=1#gref

51. Costantini, A., Mancini, S., Giuliodoro, S., Butini, L., Regnery, C., Silvestri, G., & Montroni, M. (2003). Effects of cryopreservation on lymphocyte immunophenotype and function. *Journal of Immunological Methods*, *278*(1–2), 145–155. https://doi.org/10.1016/s0022-1759(03)00202-3

52. Elkord, E. (2009). Frequency of human T regulatory cells in peripheral blood is significantly reduced by cryopreservation. *Journal of Immunological Methods*, *347*(1–2), 87–90. https://doi.org/10.1016/j.jim.2009.06.001

53. Van Hemelen, D. (2016). *Characterization of allergen-specific T cell subsets in allergy: With a goal for improvement of allergen-specific immunotherapy*. Rijksuniversiteit Groningen.

54. Akadeum Life Sciences. (z.d.). *Positive Selection vs. Negative Selection: Difference Between Positive and Negative Selection | Akadeum*. Geraadpleegd op 1 juli 2022, van https://www.akadeum.com/technology/positive-selection-vs-negative-selection/#:%7E:text=Positive%20selection%20involves%20targeting%20the,cell%20type%20of%20interest%20untouched.

55. *Immunomagnetic Cell Separation: Positive Selection Vs. Negative Selection*. (z.d.). Stemcell. Geraadpleegd op 1 juli 2022, van https://www.stemcell.com/cell-separation/positive-vs-negative-selection

56. MacPherson, S., Keyes, S., Kilgour, M. K., Smazynski, J., Chan, V., Sudderth, J., Turcotte, T., Devlieger, A., Yu, J., Huggler, K. S., Cantor, J. R., DeBerardinis, R. J., Siatskas, C., & Lum, J. J. (2022). Clinically relevant T cell expansion media activate distinct metabolic programs uncoupled from cellular function. *Molecular Therapy - Methods & Clinical Development*, *24*, 380–393. https://doi.org/10.1016/j.omtm.2022.02.004

57. Leney-Greene, M. A., Boddapati, A. K., Su, H. C., Cantor, J. R., & Lenardo, M. J. (2020). Human Plasma-like Medium Improves T Lymphocyte Activation. *iScience*, *23*(1), 100759. https://doi.org/10.1016/j.isci.2019.100759

58. Palmer, C. S., Ostrowski, M., Balderson, B., Christian, N., & Crowe, S. M. (2015). Glucose Metabolism Regulates T Cell Activation, Differentiation, and Functions. *Frontiers in Immunology*, *6*. https://doi.org/10.3389/fimmu.2015.00001

59. Bettencourt, I. A., & Powell, J. D. (2017). Targeting Metabolism as a Novel Therapeutic Approach to Autoimmunity, Inflammation, and Transplantation. *The Journal of Immunology*, *198*(3), 999–1005. https://doi.org/10.4049/jimmunol.1601318

60. Pearce, E. L., Walsh, M. C., Cejas, P. J., Harms, G. M., Shen, H., Wang, L. S., Jones, R. G., & Choi, Y. (2009). Enhancing CD8 T-cell memory by modulating fatty acid metabolism. *Nature*, *460*(7251), 103–107. https://doi.org/10.1038/nature08097

61. Van Der Windt, G., Everts, B., Chang, C. H., Curtis, J., Freitas, T., Amiel, E., Pearce, E., & Pearce, E. (2012). Mitochondrial Respiratory Capacity Is a Critical Regulator of CD8+ T Cell Memory Development. *Immunity*, *36*(1), 68–78. https://doi.org/10.1016/j.immuni.2011.12.007

62. Medvec, A. R., Ecker, C., Kong, H., Winters, E. A., Glover, J., Varela-Rohena, A., & Riley, J. L. (2018). Improved Expansion and In Vivo Function of Patient T Cells by a Serum-free Medium. *Molecular Therapy - Methods & Clinical Development*, *8*, 65–74. https://doi.org/10.1016/j.omtm.2017.11.001

Appendices

1. Supplementary tables

Table 1: *antibody specifications purity panel*

Antibody mix							
Specificity	**Fluorochrome**	**Manufacturer**	**Cat #**	**Clone**	**Species**	**Concentration**	**Amount**
CD3	BV605	BD Biosciences	317322	OKT3	Mouse IgG2a, k	50 µg/ml	2.5 µl
CD8	APC-H7	BD Biosciences	560179	SK1	Mouse	200 µg/ml	2.5 µl
Cell proliferation	eFluor 670	eBiosciences					
Viability	BV510	Biolegend					
or Viability		Thermofischer					

Table 2: *antibody specifications transcription factor panel*

Antibody mix							
Specificity	**Fluorochrome**	**Manufacturer**	**Cat #**	**Clone**	**Species**	**Concentration**	**Amount**
CD3	BV605	BD Biosciences	317322	OKT3	Mouse IgG2a, k	50 µg/ml	2.5 µl
CD4	BUV395	BD Biosciences	563550	SK3	Mouse		2.5 µl
CD8	APC-H7	BD Biosciences	560179	SK1	Mouse	200 µg/ml	2.5 µl
CD45RO	FITC	BD Biosciences	555492		Mouse		7.5 µl
Cell proliferation	eFluor 670	eBiosciences					
Viability	BV510	Biolegend					
T-bet	PE-Cyanine7	eBioscience		eBio4810			5 µl
Gata3	BV711	BD Biosciences	565449		Mouse		5 µl
RORyt	PerCP-eFluor710	eBioscience		AFKJS-9			5 µl
BCL-6	BV421	BD Biosciences	563363	K112-91	Mouse		5 µl
FoxP3	PE	eBioscience		PCH101			5 µl
Helios	PE/Dazzle594	Biolegend	137232	22F6	Mouse	6 µg/ml	5 µl

Table 3: *antibody specifications activation/Treg panel*

Antibody mix							
Specificity	**Fluorochrome**	**Manufacturer**	**Cat #**	**Clone**	**Species**	**Concentration**	**Amount**
CD3	BV605	BD Biosciences	317322	OKT3	Mouse IgG2a, k	50 µg/ml	2.5 µl
CD4	BUV395	BD Biosciences	563550	SK3	Mouse		2.5 µl
CD8	APC-H7	BD Biosciences	560179	SK1	Mouse	200 µg/ml	2.5 µl
CD45RO	FITC	BD Biosciences	555492		Mouse		7.5 µl
CD25	PE-CY7	BD Biosciences		2A3	Mouse	50 µg/ml	5 µl
Cell proliferation	eFluor 670	eBiosciences					
Viability	BV510	Biolegend					
FoxP3	PE	eBioscience		PCH101			5 µl
Helios	PE/Dazzle594	Biolegend	137232	22F6	Mouse	6 µg/ml	5 µl

Table 4: *antibody specifications intracellular cytokine panel*

Antibody mix							
Specificity	**Fluorochrome**	**Manufacturer**	**Cat #**	**Clone**	**Species**	**Concentration**	**Amount**
CD3	BV605	BD Biosciences	317322	OKT3	Mouse IgG2a, k	50 µg/ml	2.5 µl
CD4	BUV395	BD Biosciences	563550	SK3	Mouse		2.5 µl
CD8	APC-H7	BD Biosciences	560179	SK1	Mouse	200 µg/ml	2.5 µl
CD45RO	FITC	BD Biosciences	555492		Mouse		7.5 µl
Cell proliferation	eFluor 670	eBiosciences					
Viability	BV510	Biolegend					
IFN-y	Alexa fluor 700	BD Biosciences	557995	B27	Mouse		2.5 µl
IL-4	PE-CY7	BD biosciences	500824	MP4-25D2	Rat		2.5 µl
IL-17A	BV421	Biolegend	512322	BL168	Mouse IgG1, k		2.5 µl
IL-21	PE	BD Biosciences			Mouse		2.5 µl

2. Supplementary figures

We were able to cross-validate these findings when investigating cell proliferation of microscopic images. Based on the size of the clumps of cells, we observed that the X-VIVO, Pim-1 inhibitor (sup-fig. 1B) condition showed a decrease in cell proliferation compared to the DMSO control (sup-fig. 1A). The panPim inhibitor, X-VIVO condition showed an even stronger decrease in cell proliferation compared to the DMSO control (sup-fig. 1C).

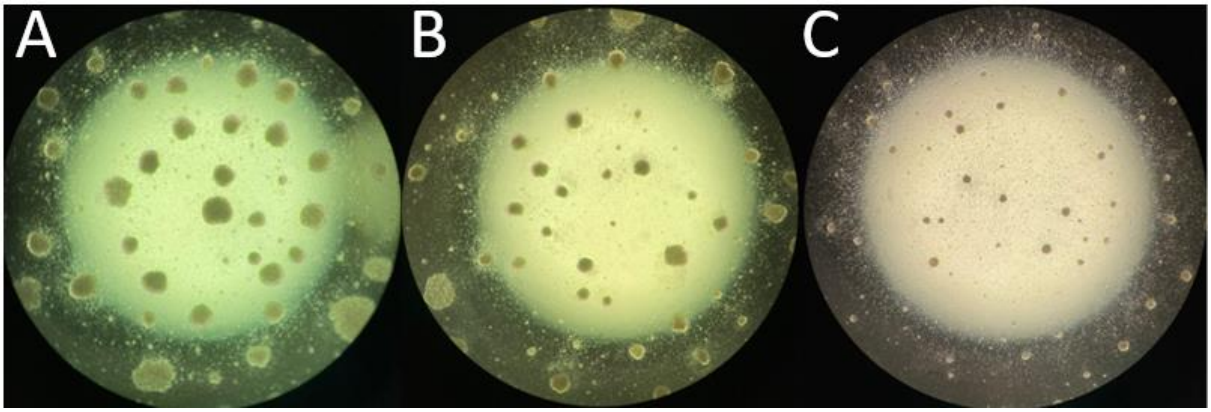

Supplementary fig 1. Cross-validation of the effect of Pim-1 kinase inhibitor (TCS PIM-1 1) and pan-Pim inhibitor (AZD1208) on CD4⁺ T cell proliferation day 6. Photomicrograph of the TCR-stimulated, DMSO treated condition after 6 days of culturing in X-VIVO + 5 % HS (A). Photomicrograph of the TCR-stimulated, Pim-1 inhibitor treated condition after 6 days of culturing in X-VIVO + 5 % HS (B). Photomicrograph of the TCR-stimulated, Pim-1 inhibitor treated condition after 6 days of culturing in X-VIVO + 5 % HS (C).

When investigating cell proliferation plots of the 6 TCR-stimulated conditions we observed a higher intensity of the generation 0 peak for the inhibitor treated conditions, suggesting a restrained proliferative capacity of the inhibitor treated CD4+ T cells. The panPim treated conditions showed a higher intensity of the generation 0 peak compared to the Pim-1 treated conditions (sup-fig. 2 & 3).

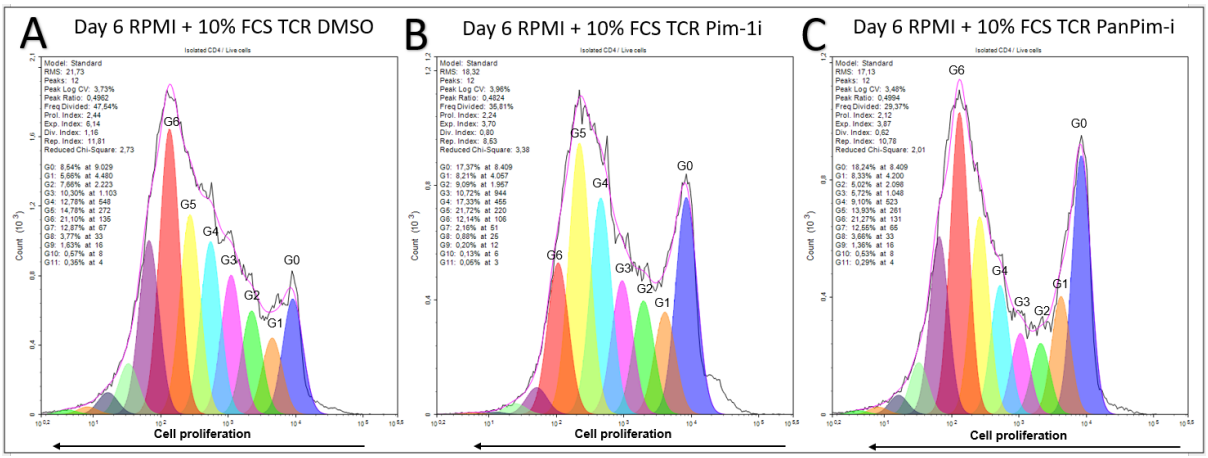

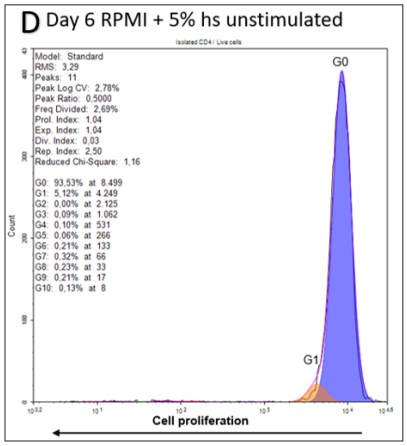

Supplementary fig. 2 Cell proliferation plots showing the effect of Pim-1 kinase inhibitor (TCS PIM-1 1) and pan-Pim inhibitor (AZD1208) on CD4⁺ T cell proliferation after 6 days of culturing in RPMI + 10% FCS. Cell proliferation plot of day 6 RPMI + 10% FCS TCR-stimulated DMSO treated condition (A). Cell proliferation plot of day RPMI + 10% FCS TCR-stimulated Pim-1 inhibitor treated condition (B). Cell proliferation plot of day RPMI + 10% FCS TCR-stimulated panPim inhibitor treated condition (C). Cell proliferation plot of day RPMI + 10% FCS unstimulated condition (D). G0 = starting generation, G1 first generation, G2 second generation, etc.

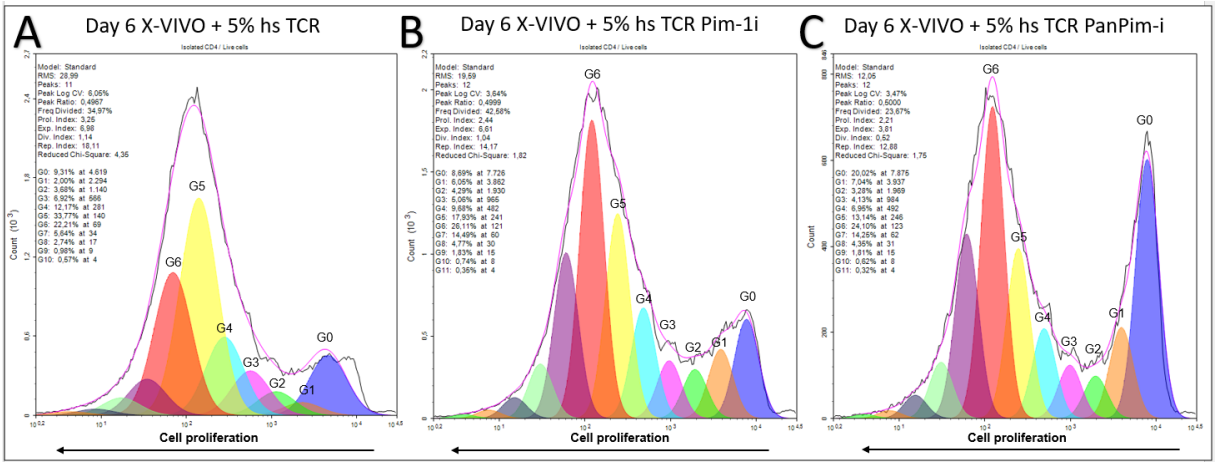

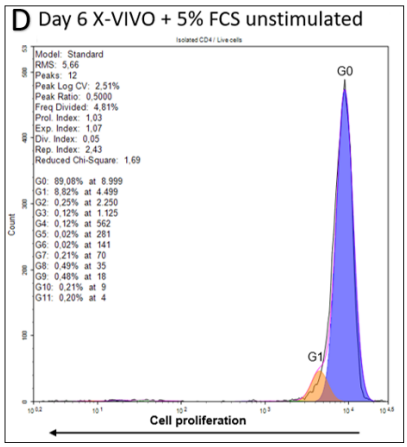

Supplementary fig 3. Cell proliferation plots showing the effect of Pim-1 kinase inhibitor (TCS PIM-1 1) and pan-Pim inhibitor (AZD1208) on CD4⁺ T cell proliferation after 6 days of culturing in X-VIVO + 5% HS. Cell proliferation plot of day 6 X-VIVO + 5% HS TCR-stimulated DMSO treated condition (A). Cell proliferation plot of day 6 X-VIVO + 5% HS TCR-stimulated Pim-1 inhibitor treated condition (B). Cell proliferation plot of day 6 X-VIVO + 5% HS TCR-stimulated panPim inhibitor treated condition (C). Cell proliferation plot of day 6 X-VIVO + 5% HS unstimulated condition (D). G0 = starting generation, G1 first generation, G2 second generation, etc.

3. Supplementary protocols

Protocol: Optimization of T cell expansion *in vitro* culture by three different medium composition

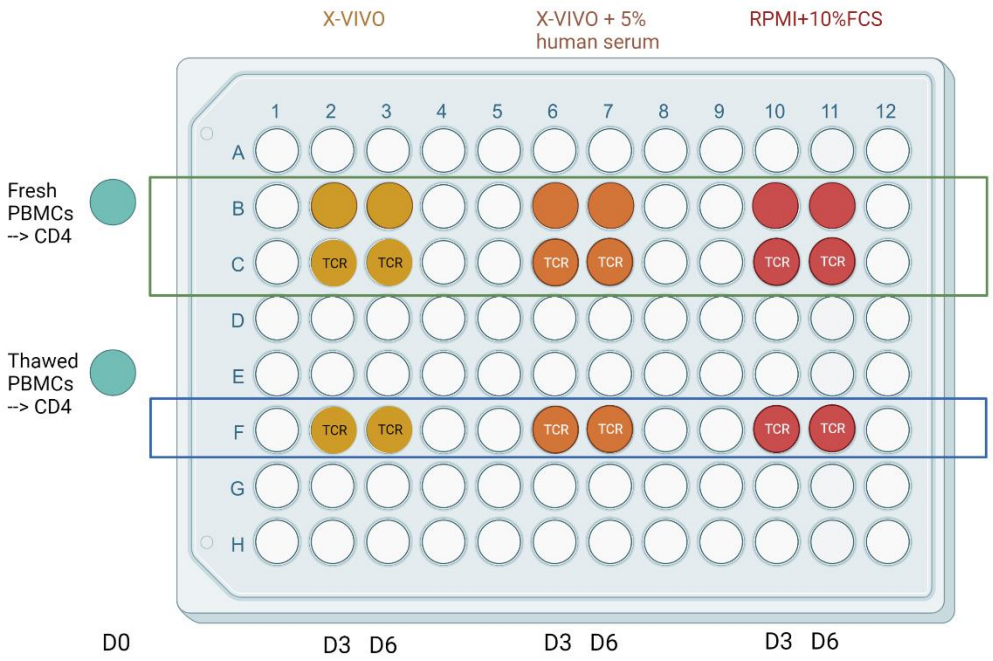

To investigate T cell phenotype (adding CD3, CD8 ab), proliferation (CPD), viability(Zombie dye)

Figure 1 Plating setup

Day -1 Coating plate with anti-CD3

(anti-CD3 OKT2: stock concentration 500 µg/mL)

1. Make solution of 100 µL PBS with 0.5 µg/ mL anti-CD3 OKT3 per well. Calculation: 2000 µl (0.5 ug/ml) = 500 ug/ml (2 µl antiCD3 stock + 1998 µl PBS)

2. Incubate the plate for 2 hours at 37°C and overnight at 4°C

Day -1 PBMCs Isolation

Place: U-Lab (primary flow or middle flow)

SOP:

1. Turning on the flow cabinet
2. Prepare workplace in flow cabinet (cleaning, checking waste, prepare materials)

Materials:

1. Fresh heparinized blood 4 tubes (approximately 40 ml)

2. Lymphoprep (warp with aluminium foil at Expire lab)
3. PBS (sterile, room temp = next to lymphoprep at Expire lab)
4. 50 ml falcon tube 2 tube
5. 10 ml isolation FACs tube (8 tubes)
6. Sero-pipette 5ml, 10 ml
7. Counting chamber (counting solution: isoton 10 ml + zap-oglobin 4 drops)

Method:

1. Pour healthy donor blood from 2 heparinized tubes into 50 ml falcon tube
2. Add PBS into the blood at ratio 1:1 (if blood is 20 ml, then add PBS 20 ml), mix it together
3. Add 4 ml of lymphoprep into each 10 ml isolation FACs tube for 5 tubes
4. Gently overlay 8 ml of diluted blood on top of 4 ml of lymphoprep *(*adjust speed of pipette gun to lower, and make a bridge of solution first)*

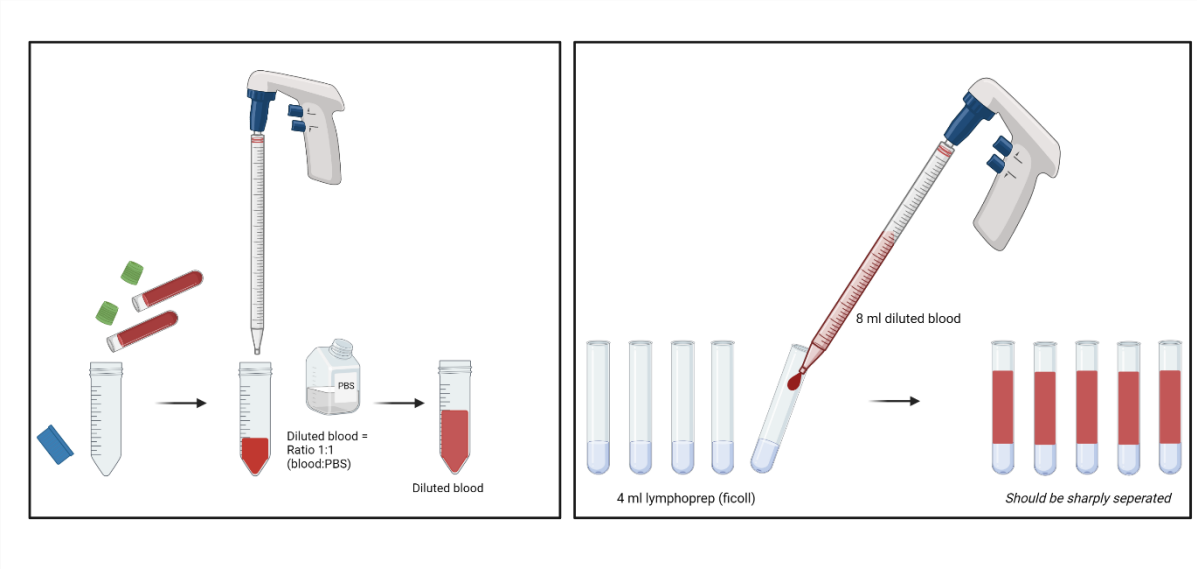

5. Centrifuge at 2400 rpm, 20 min without brake: **Prog 3**
6. Discard upper part solution by straw, until 0.5-1 cm above the PBMCs ring
7. Collect PBMCs ring into new 10 ml isolation FACs tubes (maximum 2 rings/tube)

8. Add PBS until reaching the level of 1 cm from the lid

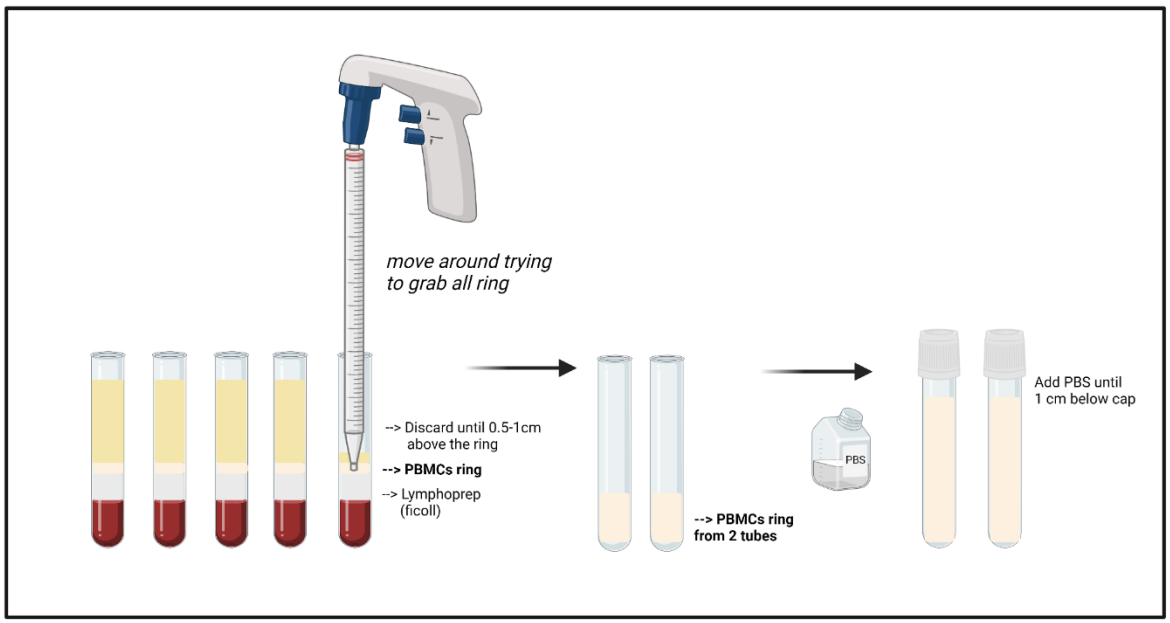

9. Centrifuge at 1800 rpm, 10 min: **Prog 2**
10. Discard supernatant as much as possible, leave at the bottom a little bit, flicking cell pellet
11. Resuspend cell pellets in each tube, pool them together in a tube of 10 ml PBS
12. Prepare counting chamber, add 40 µl of cell suspension into the chamber, count the cells
13. Centrifuge at 1200 rpm, 10 min: **Prog 1**
14. Discard all supernatant and resuspend in RPMI + 10% FCS
15. Incubate overnight at 37°C 5% CO_2

Day 0 Thawing PBMCs

Place: U-Lab (primary flow or middle flow)

SOP:

1. Turning on the flow cabinet
2. Turning on the water bath
3. Prepare workplace in flow cabinet (cleaning, checking waste, prepare materials)
4. Gather PBMCs from basement liquid nitrogen tank, sample_buffy coat 5

Materials:

1. 10 ml isolation FACs tube (3 tubes)
2. Sero-pipette 10 ml
3. Counting chamber (counting solution: isoton 10 ml + zap-oglobin 4 drops)
4. PRMI + 10% FBS (warm)

Method:

1. Fill 10 ml sero-pipet with 9 mL RPMI + 10% FCS
2. Stir frozen vial in 37°C water bath until small free moving ice cube is left

3. Use filled medium sero-pipette pipet up 1 ml of PBMCs from vial (avoid making bubble) ◊ 10 ml
4. Gently dropwise into isolation FACs tube until 4 ml left in the pipet
5. Rinse the vial with the leftover medium in the pipet in order to retrieve the last PBMCs, pipet up
6. Dropwise until finish it
7. Centrifuge 1500 rpm, 10 min, brake 5
8. Remove supernatant, resuspend the **ALL** cell pellet in 10 ml PBS, and count
9. Count:
10. Centrifuge 1500 rpm, 6 min, brake 5 and resuspend in 50 million cells/ml recommendation medium (PBS containing 2% FBS and 1 mM EDTA) for CD4 isolation.

11. Repeat step 9 and 10 for the freshly isolated PBMCs which were incubated overnight at 37°C 5% CO_2

Day 0 CD4 T cell isolation

1. Put the beads tube on the roller bank

2. Transfer solution into hard FACs tube (5 ml-size)

3. Add Isolation cocktail to sample ……. µl à (50 µl per 1 ml)
4. Mix and incubate for 5 minutes at room temp
5. Vortex RapidSpheres for 30 min
6. Add RapidSpheres to sample ……. µl à (40 µl per 1 ml) and mix
7. Add recommended medium to top up the sample to 2.5 ml, mix and gently pipetting up and down few times
8. Place tube (without lid) into the magnet and incubate for 3 minutes
9. Wait until the solution turns clear, magnet beads stick at the side of tube, then take the sample by adjusting pipette to 500ul, carefully pipet it into new 5ml soft FACs tube without disturbing the beads
10. Incubate the newly acquired 5 ml tube in the magnet again, incubate for 3 min and transfer the cells to a new 5ml soft FACs

11. Take the untouched negatively selected cells into the new 5 ml FACS tube

12. Centrifuge at 1200 rpm, 10 min, brake 4 and resuspend in 2 ml warm PBS

13. Count the isolated cells

CD4 Freshly isolated PBMCs:…….. And CD4 Thawed PBMCs:……..

14. Divide 200,000 cells of each sample into hard FACs tube for purity panel check

15. Centrifuge with 1500 rpm 6 min brake 5 and resuspend cells (fresh CD4 and Thawed CD4) in warm PBS to a final concentration of **5 x 10^6/450 µL**
(or other depending on the amount of cells, see table below)

Amount of cells (x 10^6)	amount of PBS (µL)
1	90
2	180
3	270
4	360
5	450

Day 0 Cell Proliferation Dye staining

1. Prepare warm RPMI + 10% FCS

2. Dilute 1 µL of 5 mM/ml of CPD in 499 µL PBS to an end concentration of 10 µM/ml

3. Keep cells in 37°C water bath for 5 minutes

4. Add diluted CPD to the cell suspension (1:10, end concentration 1 µM/ml)

5. Incubate in 37°C water bath for 10 min at dark, while mixing gently every 2 min

6. Stop labeling by adding 4-5 volumes of complete media (RPMI+10%FCS)

7. Wash cells with complete media, centrifuge at 1500 rpm, 6 min brake 5

8. Wash cells once with RPMI+10% FCS

9. Resuspend the cells both CD4 freshly isolated and CD4 thawed in PBS, count and divide 200.000 cells for each condition for day 0 purity panel

10. Divide the rest of the cells for each condition (freshly isolated and thawed) in 3 5 ml FACS tubes

11. Centrifuge at 1500 rpm, 6 min brake 5.

12. resuspend for each condition 1 5 ml FACS tube in X-VIVO, 1 5 ml FACS tube in X-VIVO + 5% human serum and 1 5 ml FACS tube in RPMI + 10 % FCS to a final concentration of $2x10^6$ cells/ml.

Day 0 Plate washing

Wash wells of plates 2 times with PBS

Day 0 Cell seeding and stimulation

1. Divide 100 µl of the obtained cell suspensions to the corresponding well indicated in figure 1.

2. Dilute the 100 µg/ml stock anti-CD28/49d in every medium 10x and add 20 µl to every TCR stimulated well with the corresponding medium (final concentration 1 µg/ml)
3. Top the wells up with 80 µl of the medium corresponding to the medium indicated in figure 1. (e.g. cells seeded in RPMI + 10 FCS are topped up with RPMI + 10% FCS)
4. Incubate the plate for 3-6 days at 37°C 5% CO_2

Day 0 viability staining and surface marker staining

1. Add PBS 2 ml to both tubes separated earlier during CPD staining and centrifuge at 1500 rpm 6 min brake 5
2. Discard supernatant and vortex pellet briefly
3. Add 100 µl of diluted zombie dye —> incubate for 15 minutes
4. Add 2 ml of PBS+1%BSA in each tube to wash the dye (1500 rpm brake 5 6 min)
5. Discard the supernatant and leave a little for staining surface markers (CD8/CD3)
6. Add 2.5 µl CD8-APC-H7 + CD3-BV605 2.5 µl to each tube
7. Incubate for 30 minutes at dark
8. Prepare FACS lysing solution buffer 1 ml + 9 ml Demi water
9. After staining, add 1 ml of FACs lysing solution (diluted) each tube
10. Incubate 10 min at dark
11. Centrifuge at 1800 rpm brake 5 for 3 min
12. Wash once with 2 ml of PBS+1%BSA and centrifuge at 1800 rpm brake 5 for 3 min
13. Discard supernatant and resuspend in 200 µl of PBS+1%BSA and analyze on the Symphony

Day 3 and 6 collecting the cell, viability staining and surface marker staining

9 tubes:

1. Fresh X-VIVO

2. Fresh X-VIVO TCR

3. Thaw X-VIVO TCR

4. Fresh XV +5%

5. Fresh XV +5% TCR

6. Thaw XV +5% TCR

7. Fresh RPMI +10%

8. Fresh RPMI +10% TCR

9. Thaw RPMI +10% TCR

1. Check infection of the culture by looking at under microscope (Do not open the lid

outside!) + take a picture of the plate to see the color of the medium (top view)

2. Prepare PBS (warm it up to be at room temp) and prepare zombie dye (ZO CarloKevin) in my freezer —> thaw it 15 minutes at dark —> bring 1 µl of stock + 999 µl of

PBS —> protect the dye from the light * for the left of stock put it in stem cell box :)

3. Prepare FACS tube (hard tube size 5 ml - label them)

4. Harvest cells from D3 wells of each medium —> 9 tubes!

(Be careful: do not contaminate D6 well!) into each labeled FACS tubes (the volume is

around 200 µl)

5. Add 200 µl PBS to each empty well and flush (pipet up and down around the well) in

each well to make sure that you obtained most of the cells in the well!

6. Add PBS in empty well (protect evaporation) and put the plate back to incubator (no

contamination!)

7. For the harvested cell in 9 tubes —> add PBS 2 ml in each tube! And centrifuge at

1500 rpm 6 min brake 5

8. Discard supernatant and vortex pellet briefly

9. Add 100 µl of diluted zombie dye —> incubate for 15 minutes

10. Add 2 ml of PBS+1%BSA in each tube to wash the dye (1500 rpm brake 5 6 min)

12. Discard the supernatant and leave a little for staining surface markers (CD8/CD3)

13. Add CD8-APC-H7 25 µl + CD3-BV605 25 µl in FACS tube (prepare master mix)

Divide 5 µl of master mix in each tube —> 9 tubes →should be enough

14. Incubate for 30 minutes at dark

15. Prepare FACS lysing solution buffer 1 ml + 9 ml Demi water

16. After staining, add 1 ml of FACs lysing solution (diluted) each tube

17. Incubate 10 min at dark

18. Centrifuge at 1800 rpm brake 5 for 3 min

19. Wash once with 2 ml of PBS+1%BSA and centrifuge 1800 rpm brake 5 for 3 min

20. Discard supernatant and resuspend in 200 µl of PBS+1%BSA and analyze on the Symphony

Protocol: The effect of Pim-1 kinase inhibitor (TCS PIM-1 1) and pan-Pim inhibitor (AZD1208) on CD4⁺ T cell purity, viability and proliferative capacity

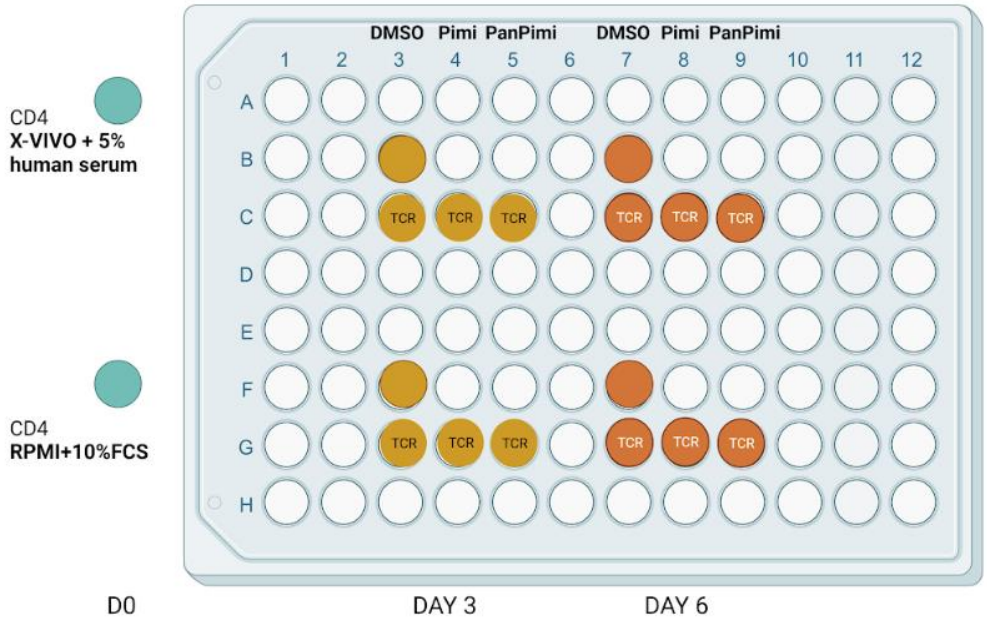

To investigate T cell phenotype (adding CD3, CD8 ab), proliferation (CPD), viability(Zombie dye)

Figure 1 Plating setup

Day -1 Coating plate with anti-CD3

(anti-CD3 OKT2: stock concentration 500 µg/mL)

1. Make solution of 100 µL PBS with 0.5 µg/ mL anti-CD3 OKT3 per well. Calculation: 2000 µl (0.5 ug/ml) = 500 ug/ml (1.5 µl antiCD3 stock + 1498.5 µl PBS)

2. Incubate the plate for 2 hours at 37°C and overnight at 4°C

Day -1 PBMCs Isolation

Place: U-Lab (primary flow or middle flow)

SOP:

3. Turning on the flow cabinet
4. Prepare workplace in flow cabinet (cleaning, checking waste, prepare materials)

Materials:

8. Fresh heparinized blood 4 tubes (approximately 40 ml)
9. Lymphoprep (warp with aluminum foil at Expire lab)
10. PBS (sterile, room temp = next to lymphoprep at Expire lab)
11. 50 ml falcon tube 2 tube

12. 10 ml isolation FACs tube (8 tubes)
13. Sero-pipette 5ml, 10 ml
14. Counting chamber (counting solution: isoton 10 ml + zap-oglobin 4 drops)

Method:

16. Pour healthy donor blood from 2 heparinized tubes into 50 ml falcon tube
17. Add PBS into the blood at ratio 1:1 (if blood is 20 ml, then add PBS 20 ml), mix it together
18. Add 4 ml of lymphoprep into each 10 ml isolation FACs tube for 5 tubes
19. Gently overlay 8 ml of diluted blood on top of 4 ml of lymphoprep *(*adjust speed of pipette gun to lower, and make a bridge of solution first)*

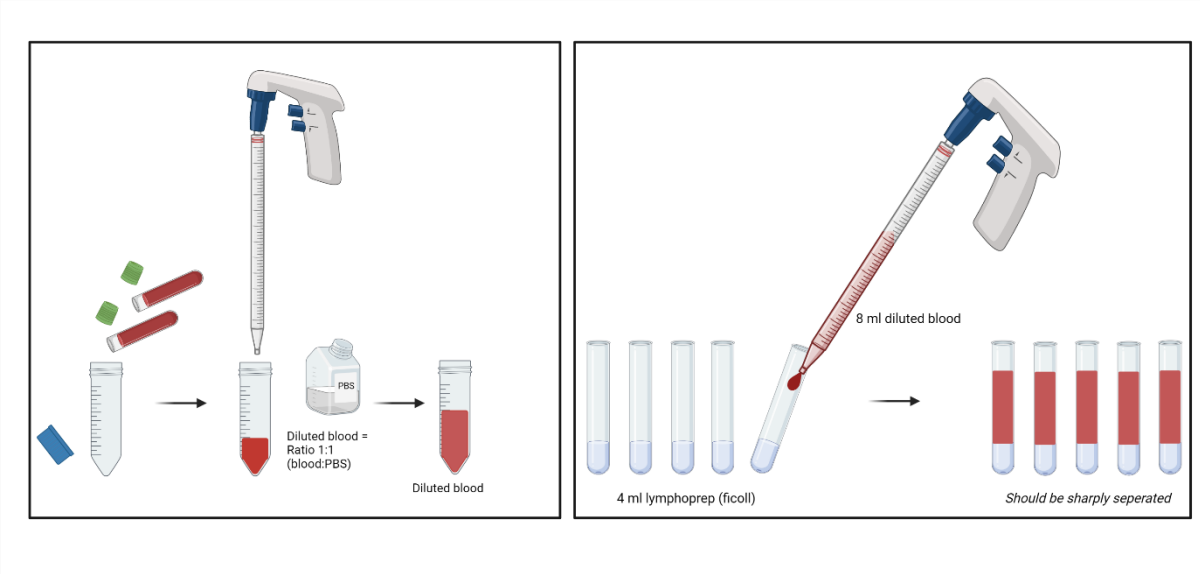

20. Centrifuge at 2400 rpm, 20 min without brake: **Prog 3**
21. Discard upper part solution by straw, until 0.5-1 cm above the PBMCs ring
22. Collect PBMCs ring into new 10 ml isolation FACs tubes (maximum 2 rings/tube)
23. Add PBS until reaching the level of 1 cm from the lid

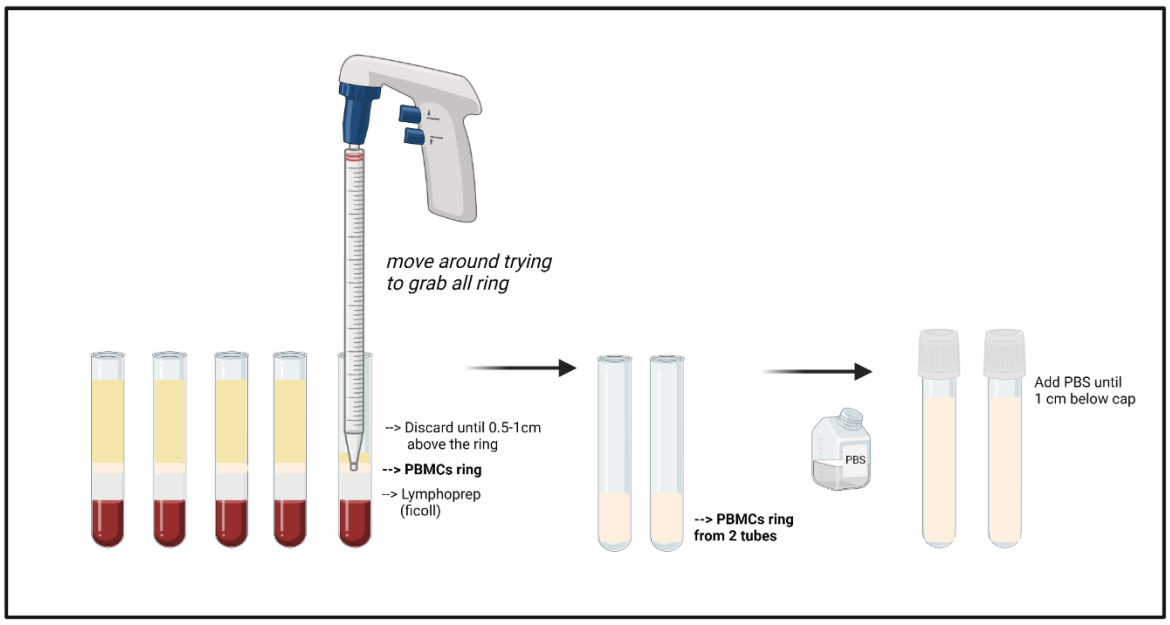

24. Centrifuge at 1800 rpm, 10 min: **Prog 2**

25. Discard supernatant as much as possible, leave at the bottom a little bit, flicking cell pellet
26. Resuspend cell pellets in each tube, pool them together in a tube of 10 ml PBS
27. Prepare counting chamber, add 40 µl of cell suspension into the chamber, count the cells
28. Centrifuge at 1200 rpm, 10 min: **Prog 1**
29. Discard all supernatant and resuspend in RPMI + 10% FCS
30. Incubate overnight at 37°C 5% CO_2

10. Centrifuge 1500 rpm, 6 min, brake 5 and resuspend in 50 million cells/ml recommendation medium (PBS containing 2% FBS and 1 mM EDTA) for CD4 isolation.

11. Repeat step 9 and 10 for the freshly isolated PBMCs which were incubated overnight at 37°C 5% CO_2

Day 0 CD4 T cell isolation

1. Put the beads tube on the roller bank

2. Transfer solution into hard FACs tube (5 ml-size)

3. Add Isolation cocktail to sample ……. µl à (50 µl per 1 ml)
4. Mix and incubate for 5 minutes at room temp
5. Vortex RapidSpheres for 30 min
6. Add RapidSphere to sample ……. µl à (40 µl per 1 ml) and mix
7. Add recommended medium to top up the sample to 2.5 ml, mix and gently pipetting up and down few times
8. Place tube (without lid) into the magnet and incubate for 3 minutes
9. Wait until the solution turns clear, magnet beads stick at the side of tube, then take the sample by adjusting pipette to 500 µl, carefully pipet it into new 5ml soft FACs tube without disturbing the beads
10. Incubate the newly acquired 5 ml tube in the magnet again, incubate for 3 min and transfer the cells to a new 5ml soft FACs

11. Take the untouched negatively selected cells into the new 5 ml FACS tube

12. Centrifuge at 1200 rpm, 10 min, brake 4 and resuspend in 2 ml warm PBS

13. Count the isolated cells

CD4 Freshly isolated PBMCs:

17. Divide 200,000 cells of each sample into hard FACs tube for purity panel check

18. Centrifuge with 1500 rpm 6 min brake 5 and resuspend cells in warm PBS to a final concentration of **5 x 10^6/450 µL**
(or other depending on the amount of cells, see table below)

Amount of cells (x 10^6)	amount of PBS (µL)
1	90
2	180
3	270
4	360
5	450

Day 0 Cell Proliferation Dye staining

1. Prepare warm RPMI + 10% FCS

2. Dilute 1 µL of 5 mM/ml of CPD in 499 µL PBS to an end concentration of 10 µM/ml

3. Keep cells in 37°C water bath for 5 minutes

4. Add diluted CPD to the cell suspension (1:10, end concentration 1 µM/ml)

5. Incubate in 37°C water bath for 10 min at dark, while mixing gently every 2 min

6. Stop labeling by adding 4-5 volumes of complete media (RPMI+10%FCS)

7. Wash cells with complete media, centrifuge at 1500 rpm, 6 min brake 5

8. Wash cells once with RPMI+10% FCS

9. Resuspend the cells in PBS, count and divide 200.000 cells for each condition for day 0 purity panel

10. Divide the rest of the cells in 2 5 ml FACS tubes

11. Centrifuge at 1500 rpm, 6 min brake 5.

12. resuspend 1 5 ml FACS tube in X-VIVO + 5% human serum and 1 5 ml FACS tube in RPMI + 10 % FCS to a final concentration of 2x10^6 cells/ml.

Day 0 Plate washing

Wash wells of plates 2 times with PBS

Day 0 Cell seeding and stimulation

5. Divide 100 µl of the obtained cell suspensions to the corresponding well indicated in figure 1.
6. Dilute the 100 µg/ml stock anti-CD28/49d in every medium 10x and add 20 µl to every TCR stimulated well with the corresponding medium (final concentration 1 µg/ml)

7. Dilute Pim1 inhibitor (prepare 10 rxn; 20 µl per rxn) →Stock 1000X → diluted 100 times (2 µl + 198 µl) → Add 20 µl of diluted into indicated wells in figure 1.
8. Dilute PanPim inhibitor (prepare 10 rxn; 2 ul per rxn) → Stock 1000X → diluted 100 times (2 µl + 198 µl) → Add 20 µl of diluted into indicated wells in figure 1
9. Dilute DMSO 2 µl + 198 µl → Add 20 µl of diluted in each well indicated in figure 1
10. Besides the 100 ul cells, 20 µl CD28, 20 µl inhibitors → top up each well with 60 µl of the corresponding medium (e.g. cells seeded in RPMI + 10 FCS are topped up with RPMI + 10% FCS)
11. Incubate the plate for 3-6 days at 37°C 5% CO_2

Day 0 viability staining and surface marker staining

14. Add PBS 2 ml to the tube separated earlier during CPD staining and centrifuge at 1500 rpm 6 min brake 5
15. Discard supernatant and vortex pellet briefly
16. Add 100 µl of diluted zombie dye —> incubate for 15 minutes
17. Add 2 ml of PBS+1%BSA in each tube to wash the dye (1500 rpm brake 5 6 min)
18. Discard the supernatant and leave a little for staining surface markers (CD8/CD3)
19. Add 2.5 µl CD8-APC-H7 + CD3-BV605 2.5 µl to each tube
20. Incubate for 30 minutes at dark
21. Prepare FACS lysing solution buffer 1 ml + 9 ml Demi water
22. After staining, add 1 ml of FACs lysing solution (diluted) each tube
23. Incubate 10 min at dark
24. Centrifuge at 1800 rpm brake 5 for 3 min
25. Wash once with 2 ml of PBS+1%BSA and centrifuge at 1800 rpm brake 5 for 3 min
26. Discard supernatant and resuspend in 200 µl of PBS+1%BSA and analyze on the Symphony

Day 3 and 6 collecting the cell, viability staining and surface marker staining

8 tubes:

1. X-VIVO +5% human serum unstimulated

2. X-VIVO +5% human serum TCR DMSO

3. X-VIVO +5% human serum TCR Pim-1i

4. X-VIVO +5% human serum TCR PanPim-i

5. RPMI + 10% FCS unstimulated

7. RPMI +10% FCS TCR DMSO

8. RPMI +10% TCR TCR Pim-1i

9. RPMI +10% FCS TCR PanPim-i

1. Check infection of the culture by looking at under microscope (Do not open the lid outside!) + take a picture of the plate to see the color of the medium (top view)

2. Prepare PBS (warm it up to be at room temp) and prepare zombie dye —> thaw it 15 minutes at dark —> bring 1 µl of stock + 999 µl of

PBS —> protect the dye from the light * for the left of stock put it in stem cell box :)

3. Prepare FACS tube (hard tube size 5 ml - label them)

4. Harvest cells from D3 wells of each medium —> 8 tubes!

(Be careful: do not contaminate D6 well!) into each labeled FACS tubes (the volume is around 200 µl)

5. Add 200 µl PBS to each empty well and flush (pipet up and down around the well) in each well to make sure that you obtained most of the cells in the well!

6. Add PBS in empty well (protect evaporation) and put the plate back to incubator (no contamination!)

7. For the harvested cell in 8 tubes —> add PBS 2 ml in each tube! And centrifuge at 1500 rpm 6 min brake 5

8. Discard supernatant and vortex pellet briefly

9. Add 100 µl of diluted zombie dye —> incubate for 15 minutes

10. Add 2 ml of PBS+1%BSA in each tube to wash the dye (1500 rpm brake 5 6 min)

12. Discard the supernatant and leave a little for staining surface markers (CD8/CD3)

13. Add CD8-APC-H7 25 µl + CD3-BV605 25 µl in FACS tube (prepare master mix)

Divide 5 µl of master mix in each tube —> 8 tubes →should be enough

14. Incubate for 30 minutes at dark

15. Prepare FACS lysing solution buffer 1 ml + 9 ml Demi water

16. After staining, add 1 ml of FACs lysing solution (diluted) each tube

17. Incubate 10 min at dark

18. Centrifuge at 1800 rpm brake 5 for 3 min

19. Wash once with 2 ml of PBS+1%BSA and centrifuge 1800 rpm brake 5 for 3 min

20. Discard supernatant and resuspend in 200 µl of PBS+1%BSA and analyze on the Symphony